Infiltration of Spilled Oil in Soil under Various Environmental Conditions

Zhaonian Qu

A Thesis
in
The Department
of
Building, Civil and Environmental Engineering

Presented in Partial Fulfillment of the Requirements
for the Degree of Master of Applied Science (Civil Engineering) at
Concordia University
Montreal, Quebec, Canada

August 2023

CONCORDIA UNIVERSITY

School of Graduate Studies

This is to certify that the thesis prepared

By: Zhaonian Qu

Entitled: Infiltration of Spilled Oil in Soil under Various Environmental Conditions

and submitted in partial fulfillment of the requirements for the degree of

Master of Applied Science (Civil Engineering)

Complies with the regulations of the University and meets the accepted standards with respect to originality and quality.

Signed by the final examining committee:

Dr. Zhi Chen Chair

Chair's name

Dr. Biao Li Examiner

Examiner's name

Dr. Zhi Chen Examiner

Examiner's name

Dr. Chunjiang An Supervisor

Examiner's name

Approved by Dr. Chunjiang An

Chair of Department or Graduate Program Director

____________ 2023 Dr. Mourad Debbabi

Dean of Faculty

Abstract

Infiltration of Spilled Oil in Soil under Various Environmental Conditions

Zhaonian Qu

Inland oil spills are environmental accidents that have significant impacts on environmental and ecological health. Inland spill pollution in the soil may pose a particular challenge. To achieve a fast response, the oil transport mode such as infiltration should be well understood. Herein, in this thesis, the comprehensive literature review was firstly conducted to study the cause, transport, and impact of spilled oil, as well as the response techniques for spill incidents. Secondly, the new features of oil penetration were revealed in thawing frozen soil under various weather conditions. The results showed the penetration behavior of spilled oil in the thawing frozen soil and the influence of salinity level. The modified Green-Ampt model could simulate the penetration process well especially with high water content, relatively cold temperature, and slow thawing rate. Thirdly, the infiltration behavior of water-in-oil emulsions and the influencing factors were investigated by assessing the characteristics of different emulsions. The experiment results showed that an increase of water and fine particle content and decrease in temperature would improve the viscosity of emulsions and reduce the infiltration rate, whereas salinity levels had a negligible impact on infiltration if the pour point of emulsion systems was far higher than the freezing point of water droplets. Fourthly, this study indicate that the presence of nettings and plant roots has a considerable impact on the oil infiltration process in various soils. The findings of this study can help improve the emergent response of inland oil spills.

ACKNOWLEDGEMENTS

I would like to express my heartfelt gratitude to my supervisor, Dr. Chunjiang An. I am immensely thankful to him for his attentive guidance and unwavering support throughout my master's program. I consider myself fortunate to have such an exceptional mentor who has always provided me with prompt, sound, and well-suited advice for both my academic pursuits and personal growth. Dr. An's encouragement has been instrumental in shaping my academic journey, and he has instilled in me the courage and confidence to pursue a Ph.D. program after completing my current master's degree.

I also give my hearty thanks to my friends and colleagues in Concordia University for their assistance in various aspects of my research and for their support with constant friendship.

Lastly, I want to express my deepest gratitude to my parents for their unwavering support and constant encouragement throughout my years of study and the process of researching and writing this thesis. Their love and encouragement have been the driving force behind my academic journey, and I am truly grateful for their sacrifices and belief in me. This achievement would not have been possible without their guidance and presence in my life. I am forever thankful to my parents for being my pillars of strength and motivation.

Table of Contents

LIST OF TABLES vii
LIST OF FIGURES viii
CHAPTER 1. INTRODUCTION 1
CHAPTER 2. LITERATURE REVIEW 4
2.1 Inland oil spill accidents 4
2.2 Behavior and fate of inland spilled oil 5
2.3 Contamination of inland oil spills 7
2.4 Response techniques of inland oil spills 10
CHAPTER 3. AN EXPERIMENTAL AND MODELING STUDY ON THE PENETRATION OF SPILLED OIL INTO THAWING FROZEN SOIL 13
3.1. Background 13
3.2. Materials and methods 15
3.2.1. Materials 15
3.2.2. Experimental setup and procedure 15
3.2.3. Penetration model **..... 17**
3.3. Results and discussion 18
3.3.1. Temperature and viscosity changes in the thawing process 18
3.3.2. Penetration depth of oil in thawing frozen soil 19
3.3.3. Oil concentrations at different depths during the thawing process 22
3.3.4. Effect of salinity on oil penetration 24
3.3.5. Modeling of oil penetration in thawing frozen soil 27
3.4. Summary 30
CHAPTER 4. ASSESSMENT OF THE INFILTRATION OF WATER-IN-OIL EMULSION INTO SOIL AFTER SPILL INCIDENTS 32
4.1. Background 32
4.2. Materials and methods 34
4.2.1. Materials 34
4.2.2. Emulsion preparation 34
4.2.3. Microscopy and droplet size determination 35
4.2.4. Viscosity and thermal behavior analysis 35

4.2.5. Column infiltration experiments 35
4.3. Results and discussion 36
4.3.1. Characteristics of different emulsions 36
4.3.2. Effect of temperature and water cut on infiltration 40
4.3.3. Oil concentration of different soil layers during infiltration 44
4.3.4. Effect of salinity level on emulsion infiltration 46
4.3.5. Impact of solid particles on infiltration behavior 48
4.3.6. Simulation of emulsion infiltration processes 50
4.4. Summary 52
CHAPTER 5. THE IMPACT OF PLANT ROOTS ON THE INFILTRATION PROCESS IN INLAND OIL SPILL ACCIDENTS 54
5.1. Background 54
5.2. Materials and methods 54
5.2.1. Materials 55
5.2.2. Experiment procedures 55
5.3. Results and discussion 56
5.3.1. Effect of nettings with various mesh sizes on infiltration 56
5.3.2. Oil Concentration of Different Soil Layers During Infiltration 58
5.4. Summary 61
CHAPTER 6. CONCLUSIONS 62
6.1. Summary 62
6.2. Recommendations for future research 62
REFERENCES 62
PUBLICTIONS 80

LIST OF TABLES

Table 2-1. Summary of select oil spills affecting surface and ground water supplies used for drinking water. 9

Table 3-1. The physical properties of selected soil and oil. 15

Table 3-2. Experiment procedure summary 16

LIST OF FIGURES

Figure 1-1. Number of medium (7-700 tonnes) and large (>700 tonnes) tanker spills from 1970-2022 2

Figure 2-1. (a) Sources of all inland oil spill; (b) Sources of larger inland oil spill; (c) types of oil in all inland oil spill; (d) types of oil in larger inland oil spill. 5

Figure 3-1. (a) The temperature change of soil during penetration; (b) The viscosity changes of oil during penetration 19

Figure 3-2. The penetration depth vs time in (a) 0% water content; (b) 5% water content; (c) 10% water content; (d) 15% water content. 21

Figure 3-3. The oil concentration in different soil layers in (a) 0% water content; (b) 5% water content; (c) 10% water content; (d) 15% water content. 24

Figure 3-4. (a) The temperature change and penetration depth of different salt contents under various temperature and thawing rates: (b) 5 °C; (c) -5 °C; (d) 0 °C; (e) Rh; and (f) Rl. (SC means salinity content) 26

Figure 3-5. The penetration depth simulated by modified Green-Ampt model of (a) 0% water content; (b) 5% water content; (c) 10% water content; (d) 15% water content. 30

Figure 4-1. Microscopy and particle size distribution of emulsions with (a) 10% water content (b) 30% water content (c) 50% water content 37

Figure 4-2. DSC images of emulsions with (a) different water content (b) 30% water content with different salinity level 38

Figure 4-3. Viscosity at different temperatures of emulsions with (a) 0% water content (b) 10% water content (c) 30% water content (d) 50% water content 40

Figure 4-4. Infiltration curves at different temperature of emulsions with (a) 0% water content (b) 10% water content (c) 30% water content (d) 50% water content 41

Figure 4-5. Oil concentration in different soil layers at different temperatures of emulsions with (a) 0% water content (b) 10% water content (c) 30% water content (d) 50% water 45

Figure 4-6. Infiltration curves of 30% water content emulsion with different salinity levels at (a) 30 ℃ (b) 23 ℃ (c) 15 ℃ 47

Figure 4-7. Infiltration curves of 30% water content emulsion with different fine particle levels at (a) 30 ℃ (b) 23 ℃ (c) 15 ℃ 49

Figure 4-8. Infiltration data and simulating curves at different temperatures of emulsions with (a) 0% water content (b) 10% water content (c) 30% water content (d) 50% water content.. 51
Figure 5-1. Infiltration curves of oil in (a) 0.6-1 mm soil with nettings of various mesh sizes at 5 cm height (b) 0.6-1 mm soil with nettings of various mesh sizes at 4.5 cm height (c) 0.6-1 mm soil with nettings of various mesh sizes at 4 cm height (d) 1-2 mm soil with nettings of various mesh sizes at 5 cm height (e) 1-2 mm soil with nettings of various mesh sizes at 4.5 cm height (f) 1-2 mm soil with nettings of various mesh sizes at 4 cm height.. 57
Figure 5-2. Oil concentration in different layers of (a) 0.6-1 mm soil with nettings of various mesh sizes at 5 cm height (b) 0.6-1 mm soil with nettings of various mesh sizes at 4.5 cm height (c) 0.6-1 mm soil with nettings of various mesh sizes at 4 cm height (d) 1-2 mm soil with nettings of various mesh sizes at 5 cm height (e) 1-2 mm soil with nettings of various mesh sizes at 4.5 cm height (f) 1-2 mm soil with nettings of various mesh sizes at 4 cm height... 60

CHAPTER 1. INTRODUCTION

In the present world, oil is one of the most important natural resources. The petroleum industry plays a significant role in driving global economic growth and enhancing human welfare (Hamilton and Wu 2014, Kujawinski et al. 2011). However, the occurrence of oil spills has also become frequent as a consequence of oil production and transportation activities (Eckle et al. 2012). Between 1970 and 2022, around 5.88 million tonnes of oil were lost due to tanker incidents worldwide. While the number of oil spills caused by tankers has considerably decreased in the past half century, there has been little change during the last decade as shown in Figure 1-1 (ITOPF 2023). These spill accidents not only are great lose for the crew members and stockholders but also pose a severe threat to the ecological system and human beings. For example, the seepage of oil into the soil would change both the properties of the soil physically and chemically, consequently affecting the composition and structure of soil microbial communities (Yang et al. 2006). This, in turn, leads to a decline in soil quality. Additionally, the movement and infiltration of soiled oil into underground aquifers pose a negative effect to the groundwater environment and human health (Yue et al. 2023a). Furthermore, Significant oil spills along shorelines result in several negative effects, including narcotic effects on marine life, oxygen depletion, reduced sunlight penetration into the water, and hypothermia in seabirds. These spills also have long-term consequences on marine ecosystems (Amir-Heidari et al. 2019, Troisi et al. 2016). Therefore, both experts and the general public still need to maintain their focus and concern to the contamination and appropriate treatment of oil spills.

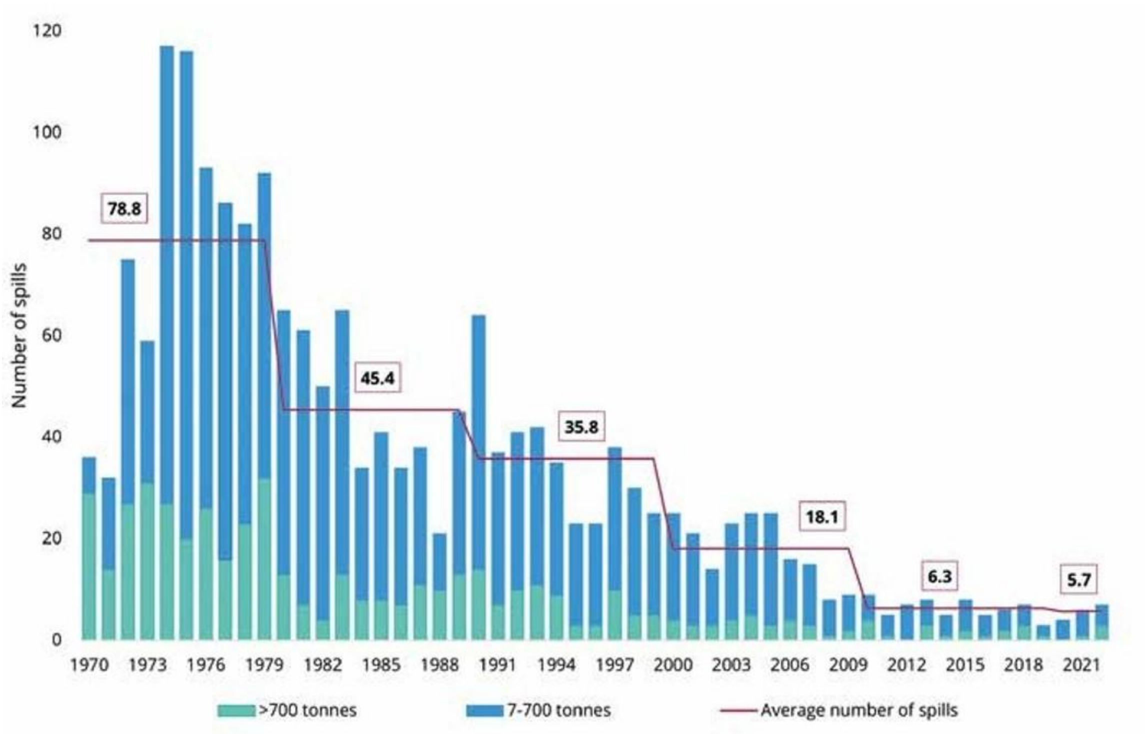

Figure 1-1. Number of medium (7-700 tonnes) and large (>700 tonnes) tanker spills from 1970-2022 (ITOPF 2023)

Recent decades, most scholars and research just focus on its negative impact on marine and coastal environment. Actually, inland oil spill accounts for most of oil spill accidents worldwide (Schmidt-Etkin 2011). Spills that occur in inland areas often have a more profound impact on sensitive environments and can significantly affect health and well-being, depending on the type of spill. In certain cases, the consequences may be even more severe compared to spills in coastal areas (Lee and Jung 2015). Hence, it is necessary to investigate the patterns and treatment methods of inland oil spill accidents. Besides, rapid oil spill response plays a fundamental role in decreasing the oil spill contamination. Oil penetration experiments and model exploration are inevitable to analyze the behavior, distribution, and transportation of oil when it spilled and penetrated into soil which are extremely necessary for making rapid response plan. Some previous studies have been conducted to investigate the infiltration behavior of aqueous and non-aqueous liquid into soil and other porous media (Zhao et al. 2015). Halmemies et al.

(2003a) studied the time periods and processes by which spilled oils and fuels penetrated different soils and found that the penetration rate is related to the soil and oil types. The more permeable the soil is, the faster the oil penetrates. Similarly, McCauley et al. (2002a) studied the infiltration rates in frozen and unfrozen soils and discovered that soil water content has a significant effect on the penetration rate. Halmemies et al. (2003a) and Grimaz et al. (2008) reported similar results and indicated that hydraulic conductivity differs between frozen and unfrozen soil. The more water soils contain, the less porosity they have, and the slower oil will penetrate. Hydraulic conductivity decreased four to five orders of magnitude in frozen soils compared with saturated unfrozen soil (Kane and Stein 1983). However, some of the special and common situations have never been studied, such as infiltration process in thawing frozen soil or the formation of water-in-oil emulsions. The missing of these situations will result in insufficient preparation of emergent response of oil spill accidents and cause severe pollution to the ecological system and local community.

Therefore, in this study, it is expected to investigate the infiltration process of spilled oil in soil comprehensively in a both theoretical and experimental way. Three objectives have been proposed as follows: (i) to conduct comprehensive literature review about the features and response technique of inland spilled oil (CHAPTER 2); (ii) to investigate the penetration process of spilled oil in thawing frozen soil under various environmental conditions (CHAPTER 3); (iii) to study the infiltration process of water in crude oil emulsions into soil columns under various conditions (CHAPTER 4); (iv) to figure out the impact of plant roots and nettings on the oil infiltration process (CHAPTER 5); A section of conclusion (CHAPTER 6) is also included in this thesis.

CHAPTER 2. LITERATURE REVIEW

2.1 Inland oil spill accidents

In order to take emergent response of inland oil spill accidents, the characteristic and features of spilled oil need to be investigated which is of great difference with oil spill in marine environment. According to Yoshioka and Carpenter (2002), spills that occur in inland areas would pose more severe contamination to the ecological system than spills in coastal areas. The extent of these impacts depends on the type of spill. Their analysis of oil spill databases reveals that 60% of all spills occurred in inland areas, while the remaining 40% took place in coastal regions. When considering spills exceeding 10,000 gallons, a staggering 88% of such incidents happened inland, with only 12% occurring in coastal areas (Brody et al. 2012). According to Stalcup et al.'s research, it is known that the minor source of spills in inland and coastal waters is pipeline spill. On the other hand, vessels, such as barges, were recognized as a significant and major source of spills in both regions (Stalcup et al. 1997). In all inland oil spill accidents, the main source is fixed facilities and vessels accounted for 39% both. Only 6% of spill accidents were from pipelines. However, in terms of larger spills (spills of 10,000 gallons or more), the main source is turned to pipelines accounted for 53.5%. The number of spills from fixed facilities were still large making up 32% of total large spill quantities. Considering the types of spilled oil, according to the ERNS data, approximately 41 percent of inland spills were attributed to fuel oil. Additionally, 20 to 22 percent of spills were related to hydraulic, transformer, and lubricating oil, while 13 to 18 percent were associated with crude oil. Moreover, about 5 to 7 percent of spills were caused by gasoline and jet fuel, with the remaining spills falling under other types of oil as shown in Figure 2-1 (Yoshioka and Carpenter 2002). However, from OSIR spill data, it is easy to observe a significantly higher amount of crude oil spills and a smaller proportion of fuel oil spills. In contrast, the majority of the larger coastal spills were attributed to fuel oil spills. From Figure 2-1, it is depicted that regarding inland spills exceeding 100,000 gallons, 40 percent of them were caused by crude oil spills from pipelines. Conversely, in the case of coastal spills, the majority of incidents were fuel oil spills originating from vessels (Zhang et al. 2019).

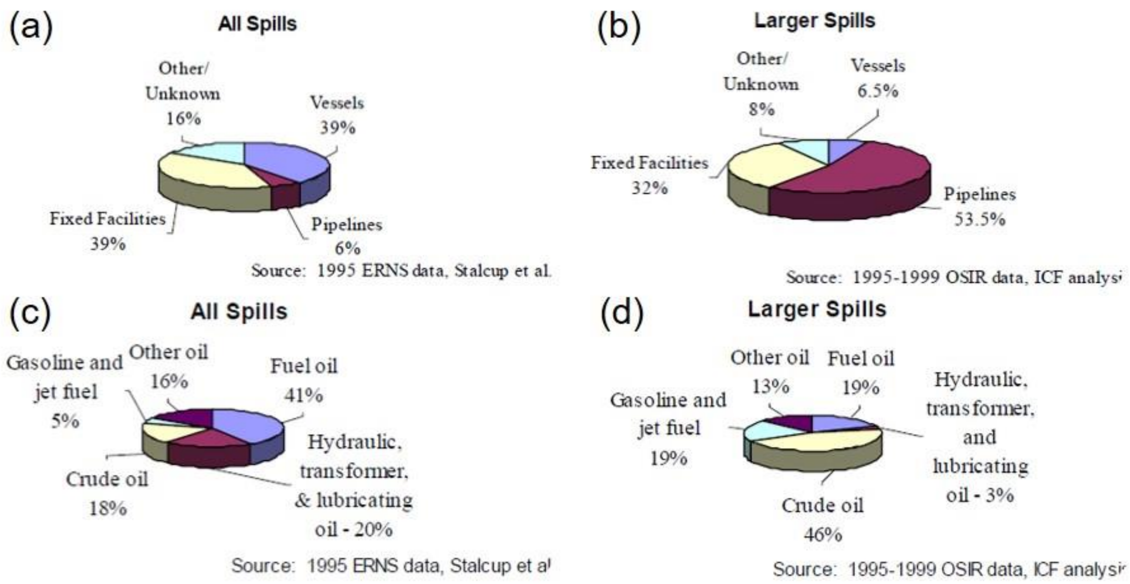

Figure 2-1. (a) Sources of all inland oil spill; (b) Sources of larger inland oil spill; (c) types of oil in all inland oil spill; (d) types of oil in larger inland oil spill (Yoshioka and Carpenter 2002)

2.2 Behavior and fate of inland spilled oil

After spill accidents occur, the spilled oil will experience various behavior and fate under different weather and location conditions (Xin et al. 2022). The most direct behavior is the movement. When the oil spills occur on land, spilled oil would spread on the land surface and infiltrate into the deep soil layer at the same time. The spreading process is mainly affected by the oil density and viscosity, land slope and plant cover, and the weather conditions like temperature and wind flow (Hussein et al. 2002). The infiltration process has also been investigated by previous experiments. Halmemies et al. (2003a) studied the time periods and processes involved in the penetration of spilled oils and fuels into various types of soils. They observed that the penetration rate is directly linked to the specific soil and oil types. In particular, they found that soils with higher permeability allowed for faster penetration of the oil compared to less permeable soils. Similarly, McCauley et al. (2002a) studied the infiltration rates in both frozen and unfrozen soils and found that soil water content plays a crucial role in determining the penetration rate of oils and fuels. The presence of soil water content was revealed to have a substantial impact on how rapidly the oils and fuels could penetrate the soil, irrespective of its frozen or unfrozen state. Halmemies et al. (2003a) and Grimaz et al. (2008) reported similar results and indicated that hydraulic conductivity varies between frozen and unfrozen soils. Higher water content in soils leads to reduced porosity, resulting in slower penetration of oil. In contrast, lower water content contributes to increased porosity, facilitating a faster rate of oil penetration. Hydraulic conductivity decreased four to five orders of magnitude in frozen soils compared with saturated unfrozen soil (Kane and Stein 1983). Some of the spilled oil could even infiltrate through soil layers and reach groundwater (Mohler et al. 2020).

Evaporation is also an important behavior of spilled oil on land (Wang et al. 2021). Hydrocarbons with short carbon chains, typically containing fewer than 12 carbon atoms, have a tendency to evaporate under natural weather conditions, particularly on warm summer days. The rate of evaporation is significantly influenced by temperature. When oil spills occur, the lighter and more volatile components of the spilled oil tend to evaporate rapidly into the air within the initial hours and days following the incident (Castiblanco et al. 2021). During the initial stage of evaporation, when the concentration of light oils in the air is very high, there is a possibility of fire hazard, which poses a significant threat to the emergency response team (French-McCay et al. 2021). After the evaporation phase, the remaining oil becomes more viscous, which can complicate response efforts. Another important process is emulsification. Many spill accidents take place at or near oil fields, riversides, and shorelines with analogous conditions of oil-water mixing. Spilled oil may meet water and it is highly likely to produce emulsions, defined as mixtures of two immiscible liquids, of which one is dispersed phase and the other one is continuous phase. The most common type of emulsion in crude oil industries is water-in-oil (W/O), which is also called “chocolate mousse” or “mousse” (Fingas and Fieldhouse 2004). Due to the high volume of injected and produced water, especially in mature oil wells, a high quantity of W/O emulsions is inevitable in oil production and transport (Abdulredha et al. 2020, Lim et al. 2015). An example is the Mingbulak oil spill, considered the fifth largest oil spill and the largest inland oil spill in history, where hundreds of thousands of tons of crude oil blew out from the oil well (Fingas 2002, Kaushik 2015).

Furthermore, other options like dissolution, photo-oxidation, sedimentation, and biodegradation are also possible for inland spilled oil. Certain hydrocarbons possess the ability to dissolve in water, but this property is primarily observed in the lighter components or polar chemicals containing elements like sulfur or nitrogen. These chemicals are still light and volatile, leading them to have a preference for evaporating rather than remaining in the water. As a result, their tendency is to escape into the atmosphere rather than staying dissolved in the water. (IPIECA and IOGP 2015). What's more, when oil spills meet sunny days, sunlight could also oxidize oil but may only affect less than 1% of spilled oil. This oxidation makes the compounds more soluble in the water (Vergeynst et al. 2019). When spilled oil encounters waters with high silt content, it also has the potential to adsorb to the surface of sediments, form Oil- Particle- Aggregates (OPA) in the water body or even sink to the bottom (Gong et al. 2014). In terms of biodegradation, it will be introduced in section 2.4 as a crucial treatment method for spilled oil.

2.3 Contamination of inland oil spills

(Oil toxic property)The EPA classifies crude oil into four categories based on their risks (EPA 2023). Class A oils, known for their high volatility and lightness, present a significant threat to both animals and human beings. They possess extremely low viscosity and tend to spread rapidly on land or water surfaces once spilled. Although their color is nearly transparent, their strong odor makes them easily detectable. Class B oils have relatively milder toxicity compared to Class A. While they can adhere to sediment surfaces, there are several methods available to remove them and mitigate pollution. On the other hand, Class C and D oils exhibit very low chemical toxicity due to their high density and viscosity. However, they can still lead to smothering and drowning of animals and plants, posing potential risks to aquatic ecosystems (Brody et al. 2012).

(Toxicity to animals and plants) Due to the oil toxicity, spilled oil can have many acute or long-term impacts on species that living in the water column like neurosensory functions and decreased fertility (Bhattacharyya et al. 2003, Green and Trett 2012) . When oil is spilled on the water surface, it can impede oxygen exchange, coat the gills of aquatic organisms, and cause pathological lesions on their respiratory surfaces. This hampers the oxygen supply and respiration of these organisms, leading to potential issues. Besides, oil can negatively affect benthic organisms living in freshwater when it settles on sediment and impede the colonization of invertebrates or cause various lethal and sublethal effects (Hoehn et al. 1974). For instance, exposure to crude Dubai oil led to 100% mortality in the benthos-dwelling isopod Asellus aquaticus, with severe toxicity observed after just a few hours at concentrations of 9.8 mg/l and above (Ramusino and Zanzottera 1986). In terms of plants, when seedlings of certain plants are exposed to oil and dispersant, they undergo various changes in growth, respiration, transpiration, and uptake of oil-based chemicals (Wilson et al. 2019). The presence of oil in the surrounding soil further stresses plant roots by hindering the oxygen supply to the roots, leading to the risk of plant death due to oxygen deprivation. Additionally, oiling on trees typically results in reduced photosynthesis in salt marsh plants, as confirmed by experimental studies (Caudle and Maricle 2014). The decrease in photosynthesis or the toxicity caused by oil leads to reduced growth and production in salt marsh plants. Consequently, oil contamination has a negative impact on the growth and productivity of these plants in salt marsh ecosystems (Caudle and Maricle 2015).

(Toxicity to drinking water and human beings) Moreover, spilled oil poses a substantial threat to the local drinking water system and can result in acute or chronic health issues for the public. Table 2-1 shows some convincing contamination cases in North America (Huang et al. 2017). Additionally, some studies have indicated that drinking water systems were contaminated in nearly half of the chemical leakage accidents that occurred in the U.S. in 2016, and approximately 60% of these incidents were associated with oil products (Weidhaas et al. 2016). The majority of crude oil products are transported through pipelines, trucks, and railways. In the unfortunate event of spill accidents during the transportation process, the polluted water may unknowingly enter the drinking water supply system. The fast movement of spilled oil can make it challenging for the local environmental protection agency to detect and prevent its entry into the drinking water supply system (Yuhua and Datao 2005). When oil enters drinking water source, the maximum contaminant concentration present in oils for regulated drinking water contaminants can be up to 2.2×10^6 times greater than the corresponding drinking water Maximum Contaminant Levels (MCLs), for example, benzo(a)pyrene (Huang et al. 2017). Indeed, even if the oil concentration is diluted by a significant amount of water, there is still a possibility of exceeding the relative standards for specific chemicals present in the oil. In the event of such an accident, thousands of people could be affected, leading to a disaster for the local community. The potential impact on public health and the environment in such scenarios is a matter of serious concern. Hence, the potential hazards of oil spills on drinking water safety must not be underestimated.

Table 2-1. Summary of select oil spills affecting surface and ground water supplies used for drinking water.

Location	Year	Pop.	Spill Details					Water System Details		
			Cause	Product	Delay, hr	Est. Vol.[a], gal	Dist., mi	Alert?	Assets	Actions
Nibley, UT	2015	5000	Truck	Diesel	na	nr	nf	No	WTP, DS, PS	Water stations in nearby cites
Mt. Carbon, WV	2015	2000	Rail	Crude: Light	na	378,000	nf	Yes	nc	Ran out; Trucked-in
Greenbrier Co., WV	2015	12,000	Truck	Diesel	na	4000	nf	Yes	WTP	Ran out; Trucked-in
Longueuil, CAN	2015	300,000	AST	Diesel	na	7500	nf	No	WTP, DS, PS	Trucked-in
Glendive, MT	2015	5500	Pipe	Crude: Light	nf	30,000	nf	No	WTP, DS, PS	Trucked-in
Lynchburg, VA	2014	492,900	Rail	Crude: Light	na	29,600	nf	Yes	nc	Alt source

Mayflower, AR	2013	_	Pipe	Crude: Heavy	12	>210,000	nf	Yes	nc	n/a
Sundre, CAN	2012	_	Pipe	Crude: Light	2.3	12,600	25	No	WTP	Trucked-in
Marshall, MI	2010	_	Pipe	Crude: Heavy	>17	>800,000	25	Yes	nc	n/a
Reston, VA	1993	1,000,000	Pipe	#2 Fuel oil	>0	477,436	60	Yes	WTP	Alt source
Simpsonville, SC	1991	10,500	Pipe	#2 Fuel oil	>0	550,000	32	Yes	WTP	Alt source; Trucked-in
Pittsburgh, PA	1988	23,000	AST	Diesel	na	>800,000	600	Yes	WTP	Alt source; Trucked-in
Atlanta, GA	1963	625,000	Pipe	Kerosene	nf	60,000	nf	No	WTP	Trucked-in

a. Volume of spilled oils are approximate values. AST = Above ground storage tank; WTP = water treatment plant; DS = Distribution system; PS = Building plumbing systems; nc = not contaminated.

2.4 Response techniques of inland oil spills

When oil spill accidents occur, the primary response is focused on oil recovery. However, the methods for recovering oil in inland spills differ from those used in marine spills (IPIECA and IOGP 2015). Large equipment like booms and skimmers may not be suitable for use in small freshwater rivers or on land surfaces (Vandermeulen and Ross 1995). In the case of inland oil spills, sorbents are commonly employed to collect and recover spilled oil on land or water surfaces, and they may be the only feasible methods for collecting oil in small spills (Ge et al. 2016). Sorbents are typically made from absorbing or adsorbing materials such as sand, clay mixtures, or straw bales due to their cost-effectiveness and straightforward application (Dhaka and Chattopadhyay 2021). Nonetheless, not all spilled oil can be fully recovered. For the remaining oil, other techniques are necessary to reduce contamination. Unlike the wide use in marine spill accidents, which rapidly dilute the oil and facilitate biodegradation, dispersants are not utilized in freshwater spills. This is because they are formulated for use in seawater and are less effective in freshwater, often exhibiting high self-toxicity in such environments (Chapman et al. 2007).

In-situ burning is also considered an effective method for reducing oil concentration in certain situations (Wang et al. 2022b). When other removal methods are limited or impractical, in-situ burning becomes a viable option. This is because in-situ burning can swiftly remove a substantial amount of spilled oil within a few hours, whereas mechanical removal methods may require a longer timeframe (Fingas 2011). Waste management also plays a role in the decision to use in-situ burning. After in-situ burning, there is minimal waste to be treated, which contrasts with mechanical removal that generates a significant amount of waste that needs proper treatment, consuming time and resources. While in-situ burning is efficient and cost-effective, some experts raise concerns about potential pollutants generated during the burning process. Emissions like carbon monoxide, sulfur dioxide, and nitrogen oxide could pose a significant threat to local communities' air quality and health (Aurell and Gullett 2010). In summary, in-situ burning is a powerful tool in certain spill scenarios due to its rapid oil removal and reduced waste management requirements. However, environmental and health considerations related to the burning process should be carefully evaluated before its implementation.

Moreover, biodegradation may not be considered an emergency response technique, but it is essential for long-term remediation of polluted soil and aquatic environments (IPIECA and IOGP 2015). Microbes are naturally present everywhere in nature. A small quantity of spilled oil can be completely degraded through microbial metabolic reactions within a few months, while a larger quantity of oil may require several years or even several decades for complete degradation (Si-Zhong et al. 2009). This timeline depends on crucial influencing factors such as nutrients, oxygen, temperature, and the amount of oil (Bragg et al. 1994). To optimize the rate of oil degradation, it is necessary to add excessive nutrients at spill sites (Venosa et al. 2010). This helps to reduce the negative impact on the soil and groundwater, facilitating the microbial degradation process (Vanloocke et al. 1975). By understanding and manipulating these factors, we can effectively improve the remediation process and minimize the environmental impact of oil spills.

To conclude, inland oil spill accidents occurred frequently in the past and caused severe risks to the ecological system and human beings. To take emergency response for inland oil spills, the movement and infiltration process need to be investigated. However, previous experiments only studied the ideal conditions and situations of oil infiltration process. The impact of special conditions like thawing process of frozen soil, emulsion formation, and plants on the infiltration process has never been studied. Therefore, in the research below, such special situations will be investigated to better understand the oil infiltration process.

CHAPTER 3. AN EXPERIMENTAL AND MODELING STUDY ON THE PENETRATION OF SPILLED OIL INTO THAWING FROZEN SOIL[1]

3.1. Background

Oil spills are significant environmental accidents that occur every year and have serious impacts on environmental and ecological health (Bi et al. 2021, Chen et al. 2021b, Ivshina et al. 2015). There are also many concerns about inland oil spills which account for most of the oil spill accidents worldwide (Yoshioka and Carpenter 2002). Oil residues in soil can result in acute and chronic toxicity for species inhabiting the soil, leading to suffocation, neurosensory disruption, behavioral and developmental abnormalities, and reduced fertility (Green and Trett 2012). Moreover, spilled oil has an obstructive effect on the groundwater system. Rapid oil spill response plays a crucial role in decreasing the contamination from oil spills. To achieve a fast response, the oil transport mode such as penetration should be well understood. The amount of contaminated soil that needs remediation is determined by the depth and rate of oil penetration. Oil penetration experiments and modeling exploration are necessary to analyze the behavior, distribution, and transport of spilled oil. The distribution of oil is another key factor. Oil concentrations may vary in different soil layers. Knowing the extent of oil contamination is required to choose the appropriate response technique.

Some studies have discussed the penetration of oil and other liquids into frozen or unfrozen soil (Amro et al. 2013, Chuvilin and Miklyaeva 2003, Halmemies et al. 2003a). Halmemies et al. (2003a) studied the time periods and processes by which spilled oils and fuels penetrated different soils and found that the penetration rate is related to the soil and oil types. The more permeable the soil is, the faster the oil penetrates. Similarly, McCauley et al. (2002a) studied the infiltration rates in frozen and unfrozen soils and discovered that soil water content has a significant effect on the penetration rate. Halmemies et al. (2003a) and Grimaz et al. (2008) reported similar results and indicated that hydraulic conductivity differs between frozen and unfrozen soil. The more water

[1] This work has been published as Qu, Z., An, C., Mei, Z., Yue, R., Zhao, S., Feng, Q., Cai, M. and Wen, J., An Experimental and Modeling Study on the Penetration of Spilled Oil into Thawing Frozen Soil. Environmental Science: Impacts and Processes (Royal Society of Chemistry), 24, 2398-2408 (2022)

soils contain, the less porosity they have, and the slower oil will penetrate. Hydraulic conductivity decreased four to five orders of magnitude in frozen soils compared with saturated unfrozen soil (Kane and Stein 1983).

However, the oil penetration process in soil that is thawing has not been investigated. Enormous amounts of land in cold regions undergo phases of freezing and thawing every year (Smith et al. 2004). In the northern hemisphere, 58 percent of the land (55 million square kilometers) freezes seasonally (Obu 2021). Under the changing climate, the increasing amount of permafrost soil will become seasonally frozen soil and start to thaw. As mentioned above, water content and porosity are the most important impact factors affecting the transport and distribution of oil in soil layers. During the thawing process, the porosity and ice-water content of soil change rapidly. Many environmental factors could affect the behaviors of pollutants like spilled oil (La and Chai 2021, Song et al. 2020a, Xin et al. 2019). Soil salt content is also essential in the oil spill and thawing process. Salt content varies a lot along the long-distance oil pipelines and road transportation. In the thawing process, it may change the wettability between soil and oil (Lebedeva et al. 2010), and the heat capacity and unfreezing point of soil (Demand et al. 2019, Yao et al. 2017). Therefore, the effect of soil salinity also needs to be considered in oil penetration during the thawing process. The water distribution is another interesting phenomenon in frozen soil. It was found that the liquid like non-aqueous phase liquids and water with nanoparticles in the soil would redistribute after freezing and thawing cycles which were affected by the physical and chemical properties of frozen soil (Chen et al. 2021a, Dou et al. 2022, Tian et al. 2014, Xu et al. 2021). So, it is necessary to study the oil penetration behavior in thawing frozen soil.

This study aims to support the response to oil spill accidents in cold regions by improving the understanding of the penetration process in thawing frozen soil, focusing on five specific aspects: (i) soil temperature and oil viscosity changes during the thawing process, (ii) oil penetration depth in the thawing frozen soil, (iii) oil concentrations in different soil layers during the thawing process, (iv) the impact of soil salt content on oil penetration during the thawing process, and (v) modeling of oil penetration in the thawing frozen soil.

3.2. Materials and methods

3.2.1. Materials

The soil was prepared according to the standard method *NY/T 1121.1*-2006. Soil samples were obtained from the McDonald campus of McGill university, a suburban area near Montreal in Canada, at a depth of 0~20 cm using cutting ring method from individual cores in a zig-zag pattern that are combined to produce a composite sample. The samples were dried in the wind and sieved using a 3-mm sieve. The bulk density of the soil samples was evaluated using the cylinder method; particle density was measured using a pycnometer; and hydraulic conductivity was determined using the permeameter falling head method.(Chitra et al. 2022, Chu and Fwa 2019) Detailed data on the soil properties are listed in Table 3-1. Engine oil (15W-40) from the Shell company was used as a representative oil (Table 3-1). Analysis-grade n-hexane was purchased from Fisher Chemical. Deionized water was used in all experiments.

Table 3-1. The physical properties of selected soil and oil.

Properties	**Soil**	**Oil**
Bulk density	1.16`	\
Particle density (g/cm^3)	2.534	\
Hydraulic conductivity (cm/s)	3.28×10^{-4}	\
Kinematic viscosity (40 °C) mm^2/s	\	118
Kinematic viscosity (100 °C) mm^2/s	\	15
Density kg/l	\	0.878
Flash point °C	\	234

3.2.2. Experimental setup and procedure

The summary of experiment procedure is listed in Table 3-2. Soil sample (8 cm height) was placed into a glass column with an 18-mm inner diameter (ID), which was ventilated at the bottom to imitate a real soil environment. The column was put in the environmental chamber (EPL-2H, ESPEC, USA) with temperature control. When the temperature reached the set value, 2.5 mL of engine oil were poured quickly onto the top of soil and started filming. During the penetration process, the temperature changes in the chamber and soil were recorded with an external thermometer. After penetration, a soil sample was dug out every 0.5 cm, and 0.3 g of sample of 0.5 cm of soil column were transported to a 20-mL glass vial. Before examining the oil concentrations in different soil layers, the soil samples in the glass vials were extracted using 15 mL of n-Hexane and filtered through a 0.22-um PTVE membrane. The concentration of oil was measured using Gas chromograph (GC 8890, Agilent Technologies Co., Ltd., USA). The chromatograph was equipped with a HP-5 (30 m × 0.320 mm × 0.25 μm) column and a flame ionization detector. The detector temperatures were maintained at 350 °C. The oven temperature was maintained at 35 °C and Helium was employed as carrier gas at 25 mL/min. The viscosity of oil was measured by the viscometer (DVNXLVTJG, AMETEK Brookfield, USA).

The experiments were performed under five different conditions: -5 °C, +5 °C, 0 °C, the high rate of thawing rising from -5 to +5 °C in 5 min (using Rh to represent this situation below), and the low rate of thawing rising from -5 to +5 °C in 1 hour (using Rl to represent this situation below) to represent five different situations respectively: frozen soil, unfrozen soil, ice and liquid water existing simultaneously and thawing rapidly, and thawing slowly. The same experiment was conducted with water contents of 0%, 5%, 10%, and 15% (weight ratio) and salt contents of 0%, 0.5%, 1%, and 1.5% (weight ratio of soil). The penetration process was recorded and filmed, and the depth measured by the scale paper fixed to the column. All experiments were conducted in duplicate, and the results were reported as the average value.

Table 2-2. Experiment procedure summary

Experiment procedure	**Details**
1. Soil sample preparation	(1.1) Four water contents: 0%, 5%, 10%, 15% (1.2) Four salinities: 0%, 0.5%, 1%, and 1.5%
2. Column preparation	(2.1) Place 8 cm height soil sample into a

	18mm-ID glass column
	(2.2) Poke some holes at the column bottom to ventilate
3. Column experiment	(3.1) Put columns in the chamber
	(3.2) Pour 2.5ml engine oil on soil
	(3.3) Film the penetration process
4. Chamber temperature control	Five temperature conditions: -5 °C, +5 °C, 0 °C, Rh, and Rl
5. Oil extraction and examination	(5.1) Divide soil column into layer every 0.5cm
	(5.2) Pick 0.3g soil with oil from each layer
	(5.3) Extract oil from 0.3g soil sample using 15mL hexane for 24h
	(5.4) Detect the oil concentration using GC-FID

3.2.3. Penetration model

A model will be used based on the Green–Ampt model with some modification (Simmons and Keller 2005). Darcy's law: $\boldsymbol{Q} = \frac{\boldsymbol{kA}}{\boldsymbol{\mu L}}\Delta\boldsymbol{p}$. According to the definition of Q:

$$\Delta \boldsymbol{p} = \boldsymbol{\rho} * \boldsymbol{g} * \boldsymbol{S_0} = \boldsymbol{\rho} * \boldsymbol{g} * \left(\boldsymbol{h} + \boldsymbol{h_f} + \boldsymbol{z}\right) \quad (3.1)$$

$$\text{and } K = \frac{\boldsymbol{k} * \boldsymbol{\rho} * \boldsymbol{g}}{\boldsymbol{\mu}} \quad (3.2)$$

$$\boldsymbol{v} * \boldsymbol{\varphi} = \frac{\boldsymbol{k}}{\boldsymbol{\mu L}}\Delta\boldsymbol{p} = \boldsymbol{K} * \frac{\boldsymbol{h}+\boldsymbol{h_f}+\boldsymbol{z}}{\boldsymbol{z}} = \boldsymbol{K} * \frac{\boldsymbol{S_0}+\boldsymbol{h_f}+(\mathbf{1}-\boldsymbol{\varphi})*\boldsymbol{z}}{\boldsymbol{z}} \quad (3.3)$$

$$\boldsymbol{\varphi} * \left(\frac{\boldsymbol{d}}{\boldsymbol{dt}}\boldsymbol{z}\right) = \boldsymbol{K} * \frac{\boldsymbol{S_0}+\boldsymbol{h_f}+(\mathbf{1}-\boldsymbol{\varphi})*\boldsymbol{z}}{\boldsymbol{z}} \quad (3.4)$$

where Q is the flow of liquid (m^3/s); v is the velocity of the liquid (m/s); f is the porosity of the solid media; A is the cross-sectional area (m^2); m is the dynamic viscosity of the liquid (Pa×s); L is the length of the sample (m); k is the permeability of the medium (m^2); Δp is the pressure drop (Pa); S_0 is the initial oil height (m); ρ is the density of the oil; g is the gravity (m/s^2); h is the height of the oil (m); h_f is the capillary suction (m); z is the penetration depth of the oil (m); and K is the conductivity (m/s). When μ and φ are constant,

$$\varphi * \left(\frac{d}{dt} z\right) = K * \frac{S_0 + h_f + (1-\varphi) * z}{z} \tag{3.4}$$

$$\frac{d\left(\frac{1-\varphi}{S_0+h_f}\right)z}{d\frac{K(1-\varphi)^2}{\varphi\, S_0+h_f}t} = \frac{1+\frac{1-\varphi}{S_0+h_f}z}{\frac{z(1-\varphi)}{S_0+h_f}} \tag{3.5}$$

$$\text{if } \eta = \frac{1-\varphi}{S_0+h_f} z \tag{3.6}$$

$$\text{and } \tau = \frac{K}{\varphi} \frac{(1-\varphi)^2}{S_0+h_f} t \tag{3.7}$$

the ordinary differential equation (ODE) would be converted to dη/dτ=(1+η)/η, solve this ODE, η-ln(η+1) =τ. Hence, the relationship between the penetration depth z and time t is obtained. When m and f are not constant but a function of time, the ODE has no analytical solution. Thus, the MATLAB ode45 solver would be used to obtain the numerical solution and plot the figures.

3.3. Results and discussion

3.3.1. Temperature and viscosity changes in the thawing process

As shown in Figure 3-1, the temperature of soil samples increased with the ambient temperature. The faster the temperature of the chamber increased, the faster the soil temperature increased. It was apparent that the temperature increased slower in soil with a higher water content. In two different rising groups, the soil with a water content of 15 % needed the longest time to finish temperature rising. The soil with 5% water content had a similar curve with dry soil. This is because higher water content soil adsorbs more heat. It is also worth noting that there is an inflection point when the soil temperature reached 0 °C, especially for the soil with water contents of 10% or 15%. The rising speed was decreasing before 0 °C but became extremely fast after 0 °C was reached. This is because when the temperature reaches 0 °C, the ice in frozen soil undergoes a phase change, with ice turning to liquid water, resulting in an extra phase transition and thus a slower temperature increase. It is found that the faster the ambient temperature rose and the higher the water content, the faster the soil would thaw. The rate at which soil temperature increased with time decreased before 0 °C, and increased after 0 °C. Figure 3-1(b) shows that the viscosity of the oil decreased as the temperature increased (the soil temperature was considered the same as the oil temperature in this study) in an approximately linear way. This result is similar to that reported in other studies (Esteban et al. 2012, Patel et al. 2018). The relationship fits the following function: viscosity = -114.14 × temperature + 1482.09, in the range of -5 to +5 °C. Viscosity is one of the parameters that changes with the soil temperature, and it is one of the most important impact factors impacting the transportation and distribution of oil in soil layers. The main resistance in the penetration progress is the adsorption force between soil and oil, which is closely related to the oil temperature. Consequently, this part of the soil thawing process and changes in oil viscosity have a significant effect on the model exploration discussed below.

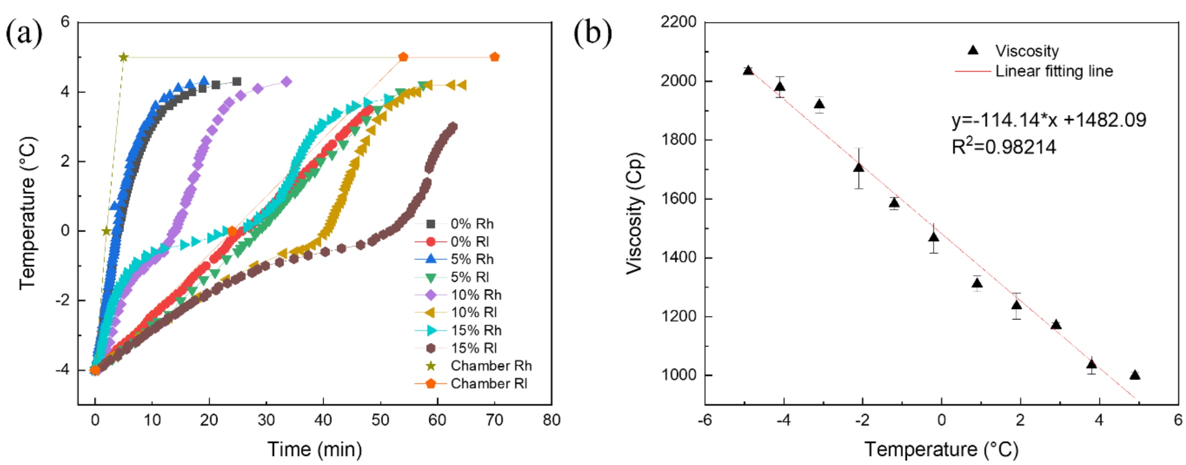

Figure 3-1. (a) The temperature change of soil during penetration; (b) The viscosity changes of oil during penetration

3.3.2. Penetration depth of oil in thawing frozen soil

It can be seen from Figure 3-2 that the penetration rate (which is the slope or first derivative of the curve in Figure 3-2 is dependent on the temperature and thawing rate.

When the temperature was high or the rate of thawing was fast, the infiltration rate was high. In the case of low temperature and a slow thawing process, it is totally converse. This is because at a relatively higher temperature the viscosity of oil is higher. As shown in Figure 3-1, the viscosity of engine oil at -5 °C is almost twice that at 5 °C (approximately 2000 Cp and 1000 Cp, respectively). Evidence of the effect of viscosity was seen in dry soil (Figure 3-2(a)). As there was no water in the soil pores, the porosity did not change, but the penetration rates at -5 °C and 5 °C differed greatly. At a higher temperature and Rh, the ice converted to liquid water more quickly than at a lower temperature and Rl, which meant the porosity was higher due to the higher unit volume of ice. Another indication of the significant effect of porosity is that oil penetrated faster in soil with lower water content irrespective of the thawing rate. In dry soil, the time it took for oil to reach 5.5 cm was less than 20 min, whereas it took 20 min, more than 20 min and almost 30 min for soil with water contents of 5%, 10%, and 15%, respectively. Moreover, at 0 °C, where ice and liquid water coexisted in the soil column, the penetration rate was between 5 min and 1 hour of the thawing rate, as most of the penetration process was finished in 30 min after 5 min thawing rate completely and before 1 hour thawing rate started to thaw.

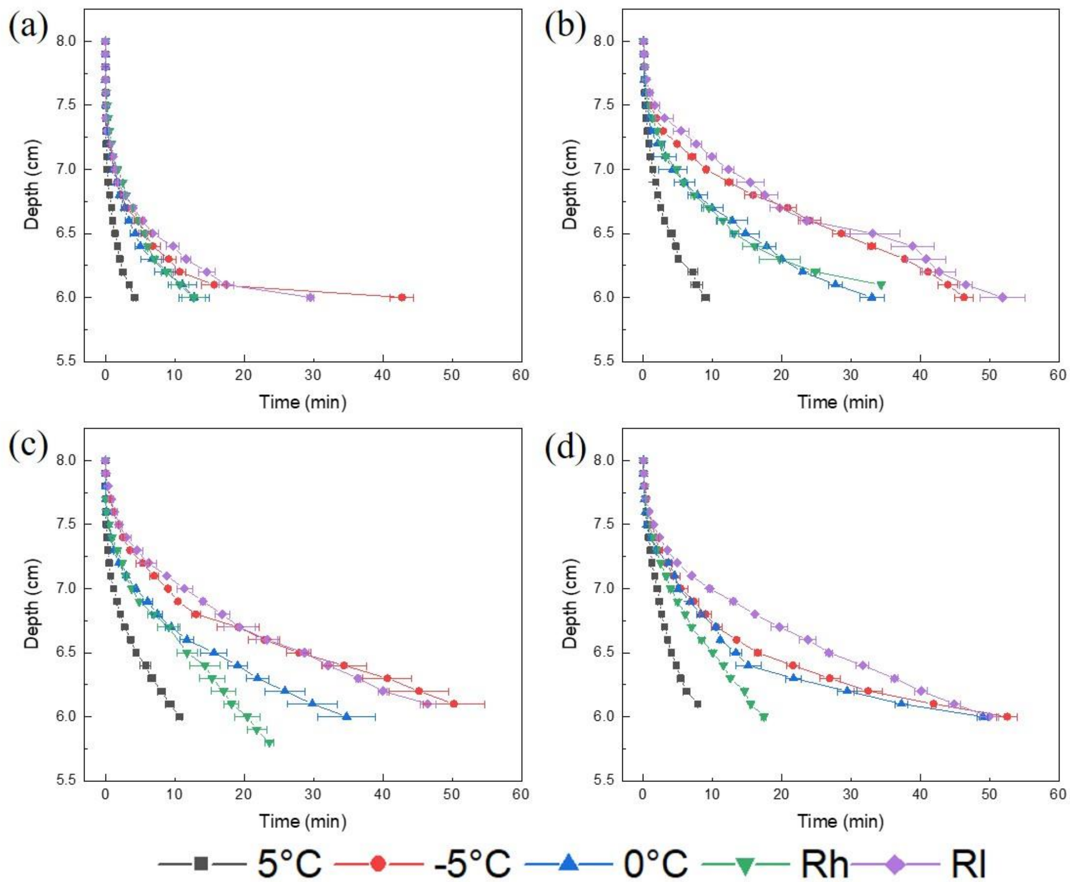

Figure 3-2. The penetration depth vs time in (a) 0% water content; (b) 5% water content; (c) 10% water content; (d) 15% water content.

In addition, the scope of the depth–time curve was slower as time increased. This phenomenon may be caused by the soil's adsorption of oil, which is the main resistance to penetration (Li et al. 2021). As more oil penetrates into the soil, the adsorption force between the oil and soil increases until the force equals that of gravity. Further, the columns used in the penetration experiments were ventilated at the bottom, so it was not high bottom air pressure that stopped the oil penetration. The lower soil under the front head remained oil free, while the higher soil retained oil or was saturated, and thus the suction capillary force assisted the penetration. Hence, the adsorption force between soil particles and oil provides the main resistance to penetration. As the temperature decreases, the viscosity of oil increases, which results in an increased adsorption force and a slower penetration rate. Comparing soil with a water content of 5% and 10% at the same temperature, the penetration rate and depth were slightly different. As noted earlier, a lower water content results in a faster penetration rate, while a higher water content leads to lower porosity and a lower penetration rate. Nevertheless, the experiments revealed that when the water content was low, the main factor affecting the penetration rate was oil viscosity in changing temperature conditions. Considering that oil penetration is blocked when the soil is saturated with water, the oil viscosity and soil water content, which affect porosity, are the two main factors affecting penetration at different temperatures. When the water content is low, viscosity is the dominant factor, and when the water content is high, porosity is the main factor. Accordingly, the response to inland oil spills should take the water content and temperature into consideration. Interestingly, the penetration rates for all states and conditions were initially similar. This could be because the oil temperature was not the same as the soil temperature, and the initial adsorption force was relatively low in the beginning. Consequently, the oil viscosity was the same in every state, resulting in the similar penetration rates.

In sum, the penetration rate is mainly determined by two factors: oil viscosity and soil porosity. During the thawing process, due to the negative correlation between viscosity and temperature and between porosity and the temperature, the penetration rate will increase as the temperature increases. In real oil spill situations, the oil penetration depth could be predicted by the temperature, soil type, and oil characteristics.

3.3.3. Oil concentrations at different depths during the thawing process

Figure 3-3 shows a chaotic picture of oil concentrations in different soil layers. This is because the sample extraction was not completely homogenous. The size distribution was heterogenous and both fine and larger particles were present, leading to different amounts of oil in samples with the same mass, and thus the sample extraction10% location and many other factors could also affect the results (Ji et al. 2021). However, some regular patterns can still be obtained. For the 5 °C and 5-min thawing process, in which there was no ice content or ice converting to water rapidly, the oil penetrated into the deeper layer. The penetration at 0 °C was similar with the 5 °C and 5-min thawing process. For the -

5 °C and 1-hour thawing process, the spilled oil tended to stay in the surface layers. In Figure 3-3, concentration 0.1% means there is 1ul engine oil in 1ml solution of oil and hexane. As noted above, the penetration process is mainly affected by viscosity and porosity, which were represented by the water and ice content in this study. In the 5 °C and 5-min thawing process, the viscosity was lowest and changed to the lowest quickly, while the porosity was largest because, for the same mass of H_2O, the liquid phase had a smaller volume. Thus, the oil penetrated faster due to gravity, capillary soil suction, and lower resistance. This was also similar at 0 °C because the initial viscosity was low and the porosity was relatively high, leading to the deeper penetration of oil; hence, the concentration of the soil columns at 0 °C was relatively uniform. As for the -5 °C and 1 hour thawing process, because of the higher volume of ice than liquid water, the porosity was lower; due to the higher viscosity, the resistance was higher. Therefore, the concentration of oil in the top layer was higher.

These results emphasize the need to pay attention to different layers of soil when spills occur depending on the time, weather, and soil type. In wintry weather (cold enough for water to freeze) and high-water content soil with low porosity, higher soil layers would retain most of the oil. In the case of a warmer temperature and low water content soil with high porosity, most of the oil would be held in the deeper soil layers. When inland oil spill accidents occur, the rapid response plan and remediation method should depend on the specific circumstances. With a high temperature and Rh, the response and remediation can focus on the whole soil column because of the uniform distribution of spilled oil. In the event of cold weather and a Rl, the soil on the top layer should be the focus because it contains most of the spilled oil (Iturbe et al. 2007, Thomas et al. 2019). This adaptability based on circumstances can significantly improve oil removal and remediation efficiency while reducing the risk of contamination.

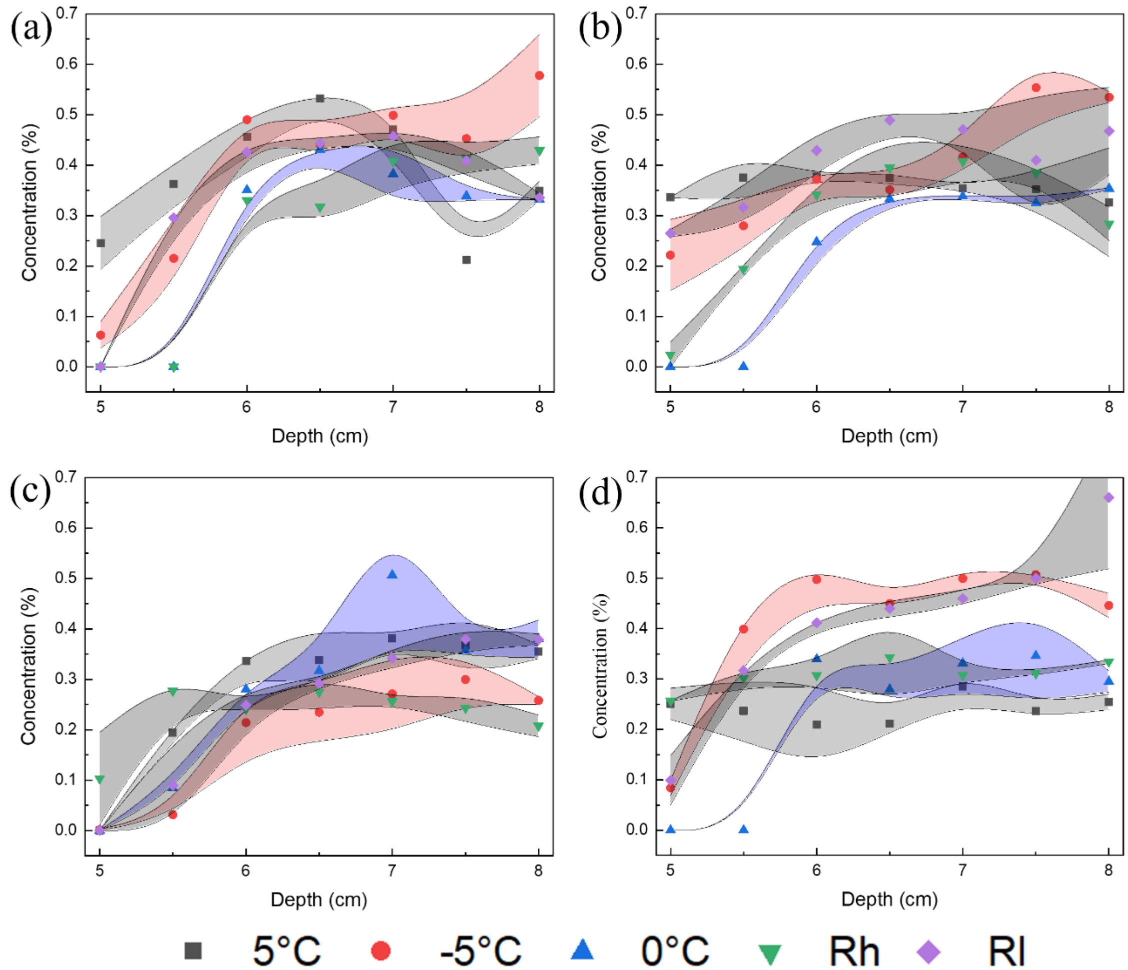

Figure 3-3. The oil concentration in different soil layers in (a) 0% water content; (b) 5% water content; (c) 10% water content; (d) 15% water content.

3.3.4. Effect of salinity on oil penetration

As shown in Figure 3-4, the temperature changes for various salinity levels were quite different. The inflection points of the curve of 0% salt content soil occurred at 0 °C for both thawing rates (Rh and Rl), as did the 0.5% salt content soil with Rl. The inflection points for other salinity and thawing rates were not obvious. It may be caused by the low heat capacity of salty water, which means less heat would be absorbed to increase same temperature (Lynn et al. 2018). This may be the reason that the temperature rising curve is straighter than 0% salt water and the temperature rising faster than it which is similar with the freezing curve (Wan et al. 2015).

As for the penetration curve (Figure 4 (b), (c), (d), (e), and(f)), it is noted that the penetration rate has no obvious difference at various salinity level. Under all kinds of conditions, no matter is the high temperature, Rh or lower temperature or Rl, the penetration rates at different salinity are almost same. The previous study reported that the increasing of salinity in soil could decrease the wettability between oil and soil, which would decrease the attraction and adhesion definitely (Lebedeva et al. 2010). This means the penetration rate was supposed to be faster in higher salt content than lower ones. Besides, the decrease of melting point of frozen soil and its interstitial water can promote the penetration rate (Demand et al. 2019). However, Chuvilin and Miklyaeva (2003) concluded from their study that the salinization of frozen soil would result in a marked decrease in oil migration. Oil migration flow (Jn) in the sample with salinization of 0.3% was $0.4\times10-8$ g/cm^2 c, which was an order lower than of in unsalinized clay, when Jn=$10.4\times10-8$ g/cm^2 c which is very significant. Therefore, the effect of salinity on the oil penetration process was expected remarkable. But the results in the present study didn't present that pattern. Demand et al. (2019) reported that the unfreezing point would be reduced owing to the salinity. It can be found in Figure 3-4 that the melting point in temperature changing curve is not obvious at all just like the 0% salt content. What is more, in the penetration depth and time figure at Rh and Rl, it is not significant either to distinguish the penetration rate in various salt content. At the 5 min rate, the oil may be infiltrated too fast to reach the melting point, but there is still no obvious gap for the lines in the figure which may be caused by the system error. As for the theory of Chuvilin and Miklyaeva (2003), we could get back to the curves of 5 and minus 5 degree. For these two cases, the temperature is constant which means the viscosity of oil and porosity of soil would not change. Therefore, the only variable is the salt content. But it is to know from Figure 3-4 that the increase of salt content means the decrease of wettability and the attraction and adhesion, while the penetration rate does not change. These theories might be not suitable for the rapid response of oil spill. Consequently, a conclusion could be obtained from this study that the salinity level does not have obvious effect on the oil penetration after oil spill under the present experimental conditions.

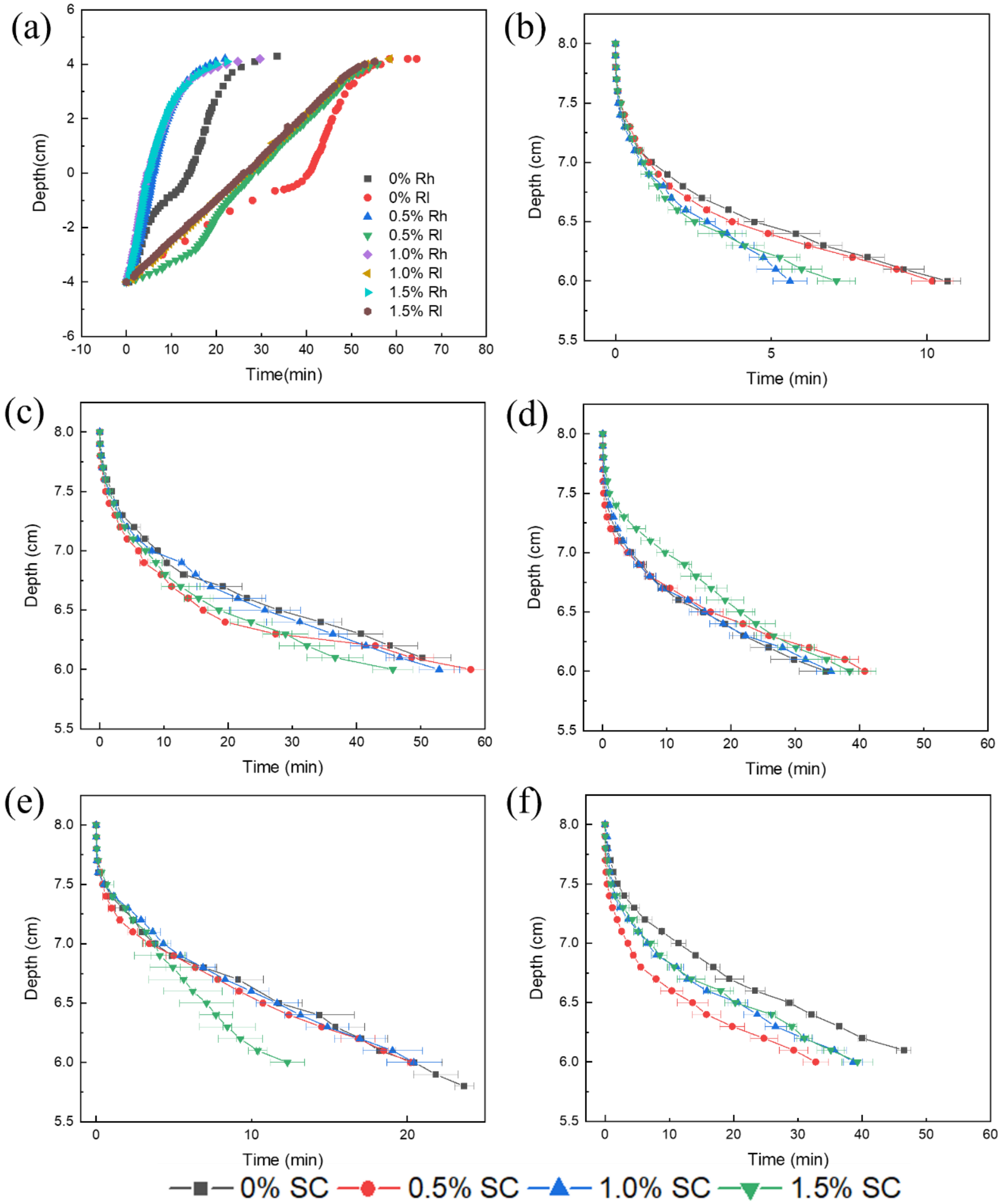

Figure 3-4. (a) The temperature change and penetration depth of different salt contents under various temperature and thawing rates: (b) 5 °C; (c) -5 °C; (d) 0 °C; (e) Rh; and (f) Rl. (SC means salinity content)

3.3.5. Modeling of oil penetration in thawing frozen soil

Environmental modeling can be used to further explore the related processes (Babamiri et al. 2021, Chen et al. 2020, Mei et al. 2021, Sundar et al. 2021). To better understand the penetration mechanism, a model will be explored based on Green-Ampt model but will be modified (Simmons and Keller 2005). This model contains parameters such as porosity, hydraulic conductivity, and water content. But some parameters like porosity are constant in this model. So according to this experiment, this model will be modified to satisfy this experiment by transforming these constant parameters to the function of time or temperature. The figure and result of the model will be compared with the column tests.

The K_{water} is known as 3.28×10^{-4} cm/s, which is equal to 1.97×10^{-2} cm/min at 25 °C. However, this conductivity was assessed for totally compacted soil sample while the column penetration experiments were conducted in uncompacted soil. Due to the fact that the compaction ratio has a significant influence on the hydraulic conductivity (Andrade 1971, Horton et al. 1994), the number needs to be modified. According to the best-fitted relationship of saturated conductivity and relative compaction (Yin 2009), the conductivity at 78% relative compaction which is the compaction ratio at column experiments is almost two orders of magnitude greater than that of 100% which is the compaction ratio at column experiments. Therefore, using the fitted relationship of the saturated conductivity and relative compaction (conductivity = 7.011 exp (-0.2034 × relative compaction)), the ratio of conductivity is 87.78. Hence, the conductivity used in this model is 3.24×10^{-4} cm/s × 87.78 = 2.84×10^{-2} cm/s. This conductivity is for water infiltrating in the soil which needs to be converted to conductivity for engine oil. $K_{oil}/K_{water} = (\rho_{oil}/\rho_{water}) \times (\mu_{water}/\mu_{oil}) = (0.878/0.997) \times (0.89/911.39) = 8.60\times10^{-4}$, therefore, K_{oil} is equal to $K_{water}\times 8.60\times10^{-4}$ which is 2.44×10^{-5} cm/s, converting to 1.46×10^{-3} cm/min. The viscosity of oil is the function of temperature according to Figure 3-1 (y=-114.14×x +1482.09) resulting the conductivity K_{oil} changes with temperature satisfying the equation K_T is equal to $\mu_5/\mu_T \times K_5 = 911.39/(= -114.14\times x + 1482.09) \times 1.46\times10^{-3}$ cm/min.

As for porosity, it is determined by the water content and ice-water conversion which is also the function of temperature. Originally, the porosity equation is $\varphi = 1- \rho_b/\rho_p$.

Considering the water content w and ice-water convention rate, the equation would be modified. When the temperature is greater than or equal to -5 °C and less than or equal to T_m which is the melting point of ice, f would be equal to 1-ρ_b/ ρ_p- w× ρ_b/ ρ_w×(r-(r-1) T/ (T_m+ 5)). When temperature is greater than T_m and less than or equal to 5 °C, f would be equal to 1- ρ_b/ρ_p - w × ρ_b/ ρ_w, where r is the volume ratio of ice to water. Therefore, for five different situations: -5 °C, +5 °C, 0 °C 5 min thawing, and 1 hour thawing, four different water contents: 0%, 5%, 10%, and 15%, and four different salinity levels: 0%, 0.5%, 1%, and 1.5%, these parameters would be reflected in the function. As for capillary suction h_f, according to Rawls et al. (1983), the Wetted front capillary pressure in cm of silty clay is 30.66. Besides, the conversion method of capillary suction is h_f= h_f' × (σ/σ') × (ρ'/ρ) where σ is the liquid surface tension (dynes/cm). To simplify the model, the wetted front is constant in this model which is represented by the h_f at 25 °C. The surface intention of water is 72 dynes/cm and that of 15W40 engine oil is 31 dynes/cm (Basit et al. 2018). Therefore, the wetted front of engine oil is h_f = h_f' × (σ/σ') × (ρ'/ρ) = 30.66× (31/72) ×(0.997/0.878) = 14.99 ≈ 15cm.

All the parameters have been required until now including porosity f, capillary suction h_f, conductivity K, and oil amount S_0. These parameters will be used in situations like various water contents (0%, 5%, 10%, 15%) and different salinity levels (0%, 0.5%, 1%, and 1.5%). The simulated curves are presented in Figure 3-5. It is shown that the simulated curves are more suitable for higher water content. At the same temperature and the thawing rate, the gap between the experimental data and the model is biggest in 0% water content and the gap gets smaller with water content increasing. The period when the model falls behind is the initial few min at which the experiments penetrated in a high rate. For instance, the oil fell almost one centimeter in the first 30 seconds under the condition of 0% water content and 5 °C. This phenomenon is common in all experiments which may be slower than 0% water content and 5 °C but still fast enough compared with the simulated model. This occurrence may be resulted from two reasons. One is the viscosity of the oil spilled. When the experiment was conducted, the oil was carried from outside of the environmental chamber and poured on the top of the soil which matches the actual oil spill situation due to the fact that the temperature of the oil transported in pipeline is usually higher than the surrounding soil (Zhao et al. 2014). Consequently, when the spill happened, the viscosity of oil is exceedingly low, resulting in the fast penetration rate at the beginning. But the model did not include such temperature and viscosity change. Future study could overcome this shortage by doing more work on the heat exchange and temperature distribution of pipeline and frozen soil. Despite the high temperature at the initial penetration and the gap produced, the penetration trend and the relative penetration rate are still suitable with the actual situation, and this proved the accuracy of the modified model. The other reason of fast penetration rate at the beginning is that during the experiments, the oil was injected by a syringe to reduce the oil residue in the syringe and insure the spilled oil amount. This operation would lead to the spilled oil with an initial speed and energy which helps accelerate the penetration rate. Actually, considering the oil transported by the tanker and truck, this is also valuable to investigate. However, in this study, such initial energy cannot be quantified and thus this situation did not demonstrate in the model.

What is more, from the figure, it is easy to find the model is more agreeable with the low temperature and Rl. All the experiment data at 5 °C are of great different of the model. But for the -5 °C, 5 min thawing and 1 hour thawing, the model has satisfactory performance. This is because according to our hypothesis, the impact of the water in soil pore on the penetration is to occupy the porosity to hinder the oil penetration. The oil and water would not interact. Hence, when water is frozen for a period of time, the model set-up is affable with the actual situation. But when the water is unfrozen, the limitation of Green-Ampt model is obvious. Besides the initial temperature and energy mentioned above, the hypothesis of the model is also important. It is said assumptions of the uniform water content and the uniform pressure, along with the air compression and air counterflow are the main disadvantages (Lukyanets 2010). Consequently, some methods based on multiphase seepage were also developed (Afanas'ev and Mel'nik 2013, Grimaz et al. 2008, Skryleva et al. 2020, Xuwen et al. 2022). However, in this experiment, the main focus is about the frozen and thawing process which is suitable and convenient to use this model owing to the solid ice under freezing condition and the features of changing temperature, viscosity, porosity, and hydraulic conductivity easily. Therefore, when oil spill incidents happen, according to the local soil parameters like hydraulic conductivity and water content, and oil characteristics like density and viscosity as well as temperature, the penetration process and depth of spilled oil could be simulated using this modified Green-Ampt model with the spilled time. Hence, the spilled situation could be understood quickly, and rapid response time could be reduced significantly which is extremely helpful to reduce the oil spill pollution and protect the local soil environment.

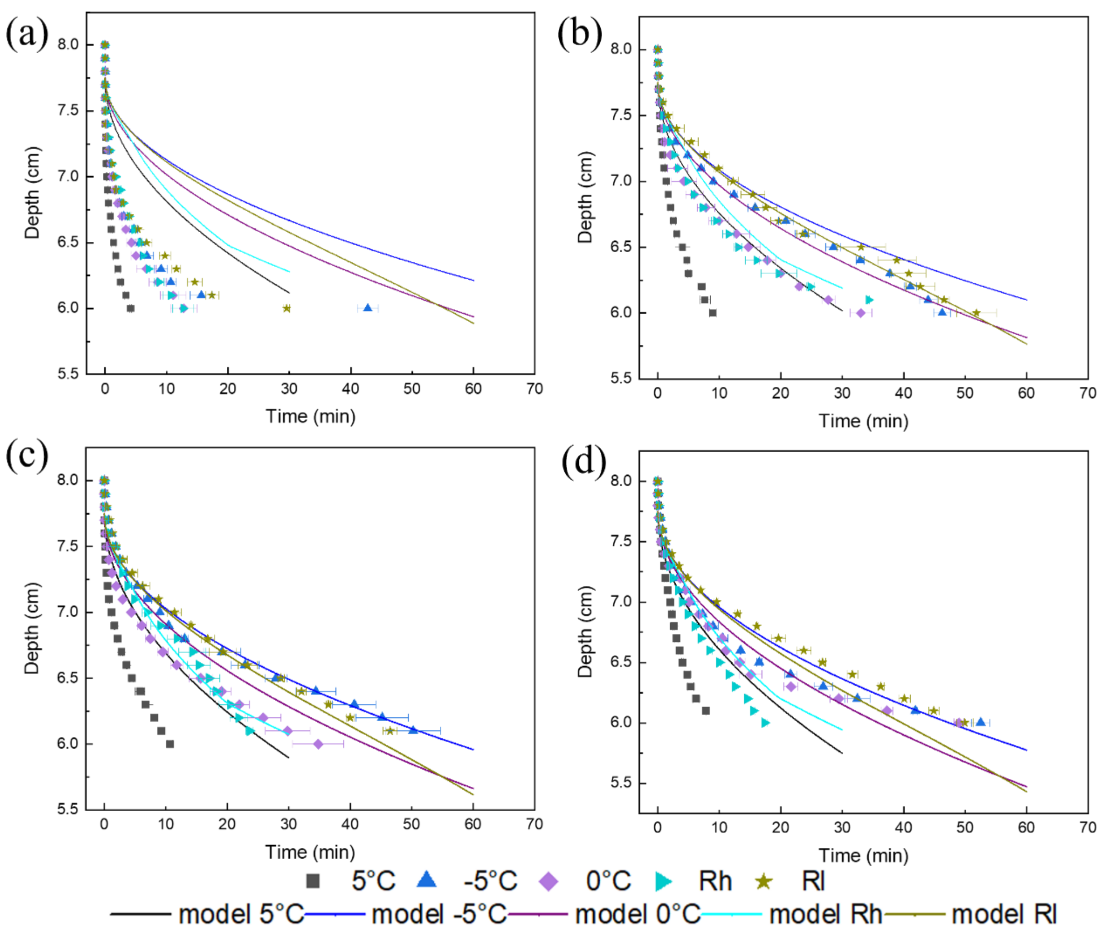

Figure 3-5. The penetration depth simulated by modified Green-Ampt model of (a) 0% water content; (b) 5% water content; (c) 10% water content; (d) 15% water content.

3.4. Summary

This is the first study to investigate the oil penetration behavior in thawing frozen soil at different temperatures and water contents. The results showed that the spilled oil tends to penetrate faster and stay in the bottom layer of soil as the temperature and thawing rate increase. Conversely, oil tends to penetrate slower and remain in the top layer as the temperature and thawing rate decrease due to the changing viscosity of oil and porosity of soil. Moreover, the salinity level has a slight influence on oil penetration process despite its theoretical impact. The modified Green-Ampt model could simulate the penetration process well especially with high water content, relatively cold temperature, and slow thawing rate. This study investigated the problem of the effect of temperature change on the oil penetration into soil including the phase transition in frozen soil. When oil spill occurs when frozen soil thaws in spring or under other temperature changing situations, responders could help determine how deep oil has reached and the relative distribution of oil in different soil layers which will be helpful for implementing response measures.

CHAPTER 4. ASSESSMENT OF THE INFILTRATION OF WATER-IN-OIL EMULSION INTO SOIL AFTER SPILL INCIDENTS[2]

4.1. Background

Oil spills are major disasters occurring every year, which can cause negative effects on ecosystems and human health (Merlin et al. 2021, Wang et al. 2021, Yue et al. 2023b). Among these accidents, many spills take place at or near oil fields, riversides, and shorelines with analogous conditions of oil-waste mixing. Spilled oil may meet water and it is highly likely to produce emulsions, defined as mixtures of two immiscible liquids, of which one is dispersed phase and the other one is continuous phase. The most common type of emulsion in crude oil industries is water-in-oil (W/O), which is also called "chocolate mousse" or "mousse" (Fingas and Fieldhouse 2004). Due to the high volume of injected and produced water, especially in mature oil wells, a high quantity of W/O emulsions is inevitable in oil production and transport (Abdulredha et al. 2020, Lim et al. 2015). An example is the Mingbulak oil spill, considered the fifth largest oil spill and the largest inland oil spill in history, where hundreds of thousands of tons of crude oil blew out from the oil well (Fingas 2002, Kaushik 2015). Furthermore, according to the data for 31,481 unconventional oil and gas (UOG) wells from 2005 to 2014 in Colorado, New Mexico, North Dakota, and Pennsylvania, 2−16% of wells reported a spill each year (Patterson et al. 2017). After spills happen, the infiltration of emulsions into soil is unavoidable. Therefore, it is critical to explore the oil infiltration process for improving spill response.

Some previous studies have been conducted to investigate the infiltration behavior of aqueous and non-aqueous liquid into soil and other porous media (Zhao et al. 2015). For example, McCauley et al. (2002b) compared hydraulic conductivities and infiltration rates of fuels in frozen and unfrozen soils. They observed that increased ice content led to

[2] This work has been published as Qu, Z., An, C., Yue, R., Bi, H., & Zhao, S., Assessment of the infiltration of water-in-oil emulsion into soil after spill incidents. Science of The Total Environment (Elsevier), 896, 165325 (2023)

a significant drop in hydraulic conductivity and infiltration rates, and sandy silty with a smaller particle size had the lowest hydraulic conductivity and infiltration rate compared with other types of soil with larger particle sizes. Qu et al. (2022) investigated the oil infiltration in thawing frozen soil with different thawing rates and water contents, and found that spilled oil tended to penetrate faster as the temperature and thawing rate increase and soil water content decreases. Other researchers drew a similar conclusion that an increase of water or ice content and the viscosity of the penetration liquid, the transformation of water to ice, and a decrease in soil particle size would result in the drop of soil porosity, leading to the reduction of infiltration rates (Amro et al. 2013, Halmemies et al. 2003b, Oghenejoboh et al. 2008). The contamination of spilled oil in soil environment was investigated too. (Jiao et al. 2021, Shen et al. 2017)

The properties of W/O emulsions, such as stability, viscosity, and droplet size distribution, are highly related to the water content of the emulsion system (Abdulredha et al. 2020, Hu et al. 2017, Liu et al. 2022). Concerning the relationship between droplet size and water content, there is the difference between the theory that higher water content with low stability results in a smaller droplet size (Abdulredha et al. 2020, Pal 1996, Zolfaghari et al. 2016) and the experimental data in some studies (Majid et al. 2015, Pang et al. 2021). This difference may be caused by the complex impact mechanism of droplet size distribution (Weiss and Muschiolik 2007). Despite the contradiction above, it is still determined that increasing the water content in an emulsion system leads to the increasing viscosity of the emulsion system and a reduction in stability. An emulsion's behavior under sub-zero temperatures is also interesting and worth studying (Hauptmann et al. 2016). Lin et al. (2008) investigated the breakage of W/O emulsions by the freeze/thaw method and found that the dispersed phase and continuous phase with different freezing points in emulsions exhibited significantly dissimilar behavior under low temperatures. Emulsions in which the dispersed phase freezes first were more stable than emulsions in which the continuous phase freezes first, in which a large number of fine gaps and crevices were produced, causing demulsification after thawing. However, despite the special mechanical and thermal features of W/O emulsions and the high risk of emulsions spilling at or near oil fields and riversides, the infiltration of emulsions into porous media such as soil is not very clear and has not been researched yet.

Therefore, in this study, the infiltration of water in crude oil emulsions into soil columns were studied under various conditions, focusing on the following aspects: (1) the infiltration rates and residue concentrations in different soil layers when emulsion spill accidents occur; (2) the influence of different influencing factors (water cut, temperature, salinity, and fine particles) on emulsion infiltration; (3) and the modeling of the infiltration process of emulsion into soil. The results can help understand the emulsion infiltration process and plan emergency responses for spill accidents.

4.2. Materials and methods

4.2.1. Materials

Soil samples were dried and sieved using 106-µm and 205-µm sieves. Particle density (2.415 g/cm^3) was measured using the pycnometer method and the bulk density was 1.254 g/cm^3. Hibernia crude oil from the Hibernia oil field southeast of St. John's, Newfoundland, Canada, was used in this study. The density of Hibernia at 20 °C is 0.854 kg/L and the pour point is 3 °C. Surface-modified montmorillonite clay (<20 µm) chosen as representative fine particles was purchased from Sigma-Aldrich, Canada. Sodium chloride and analysis-grade n-heptane were purchased from Fisher Chemical. Deionized water was used in all experiments.

4.2.2. Emulsion preparation

Emulsions with different water contents were prepared using a homogenizer (Ultra-Turrax T25, IKA, Germany). 10%, 30%, and 50% (volume) of water were added into the crude oil, respectively, drop by drop over 30 seconds while mixing it with the homogenizer at 5,000 rpm for 15 min. After the emulsion demulsified, the homogenizer was used to stir at 5,000 rpm for another 20 min to remulsify it. This method made the most stable emulsion in this experiment, and the emulsion did not separate until 48 hours. For emulsions with different salt contents, salt was dissolved in the water phase first, whereas for emulsions with different fine particle contents, montmorillonite clay was dispersed in the oil phase first.

4.2.3. Microscopy and droplet size determination

After the emulsification, the W/O emulsion was observed using an optical microscope (Omax 1600, Omax, USA). The droplet size was measured using microscopy and analyzed using the software ImageJ (National Institutes of Health, USA) to obtain the size distribution and average droplet size.

4.2.4. Viscosity and thermal behavior analysis

The viscosity of the emulsion was measured by a viscometer (DVNXLVTJG, AMETEK Brookfield, USA) at 50 rpm. For different temperatures, an environment chamber (EPL-2H, ESPEC, USA) was used to control the ambient temperature. The freezing process by which the ice formed was quantified by differential scanning calorimetry (DSC) (DSC Q20, TA Instrument, USA) to record the freezing and thawing thermal behavior considering the supercooling effect.

4.2.5. Column infiltration experiments

A soil sample (5 cm) was placed into a plastic column with a 13.5-mm inner diameter, which was ventilated at the bottom to imitate a real soil environment. The column was put into the environmental chamber with temperature control (EPL-2H, ESPEC, USA). When the temperature reached the set value, 1.0 mL of emulsion was poured quickly onto the top of soil and filming started. After the infiltration experiment, a soil sample was dug out every 0.4 cm, and 0.1 g of sample from this 0.4 cm of soil column was transported to a 20-mL glass vial. Before examining the oil concentrations in different soil layers, the soil samples in the glass vials were extracted using 10 mL of n-Hexane and filtered through a 0.22-μm PTVE membrane. The oil concentration was measured using a gas chromatograph (GC 8890, Agilent Technologies Co., Ltd., USA). The chromatograph was equipped with a DB-1 (15 m × 250 μm × 0.25 μm) column and a flame ionization detector. The detector temperature was maintained at 350 °C. The oven temperature was increased from 35 °C to 325 °C gradually, and helium was employed as a carrier gas at 25 mL/min.

The experiments were performed under four different conditions: 5 °C, 15 °C, 23 °C, and 30 °C. The same experiment was conducted with W/O emulsions with water contents of 0%, 10%, 30%, and 50% (volume ratio). WAT The penetration process was recorded and filmed, and the depth was measured using the scale paper fixed to the column. All experiments were conducted in triplicate, and the results were reported as the average value.

4.3. Results and discussion

4.3.1. Characteristics of different emulsions

As shown in Figure 4-1, the diameter of water droplets in W/O emulsions increased with the increase in water content. This is similar to the results of other studies (Pang et al. 2021). When the water content increased from 10% to 30%, although the diameter of most droplets was still below 8 μm, the maximum diameter increased from around 16 to 44 μm. When the water content reached 50%, despite the fact that the maximum diameter was less than that at 30%, the average diameter increased apparently and intuitively according to the microscopic images and size distribution statistics. These conclusions are of paramount importance since the size distribution would play a significant role in the emulsion mobility within porous media by blocking the pore throat of porous media and promoting emulsion viscosity (Soo and Radke 1986, Zolfaghari et al. 2016).

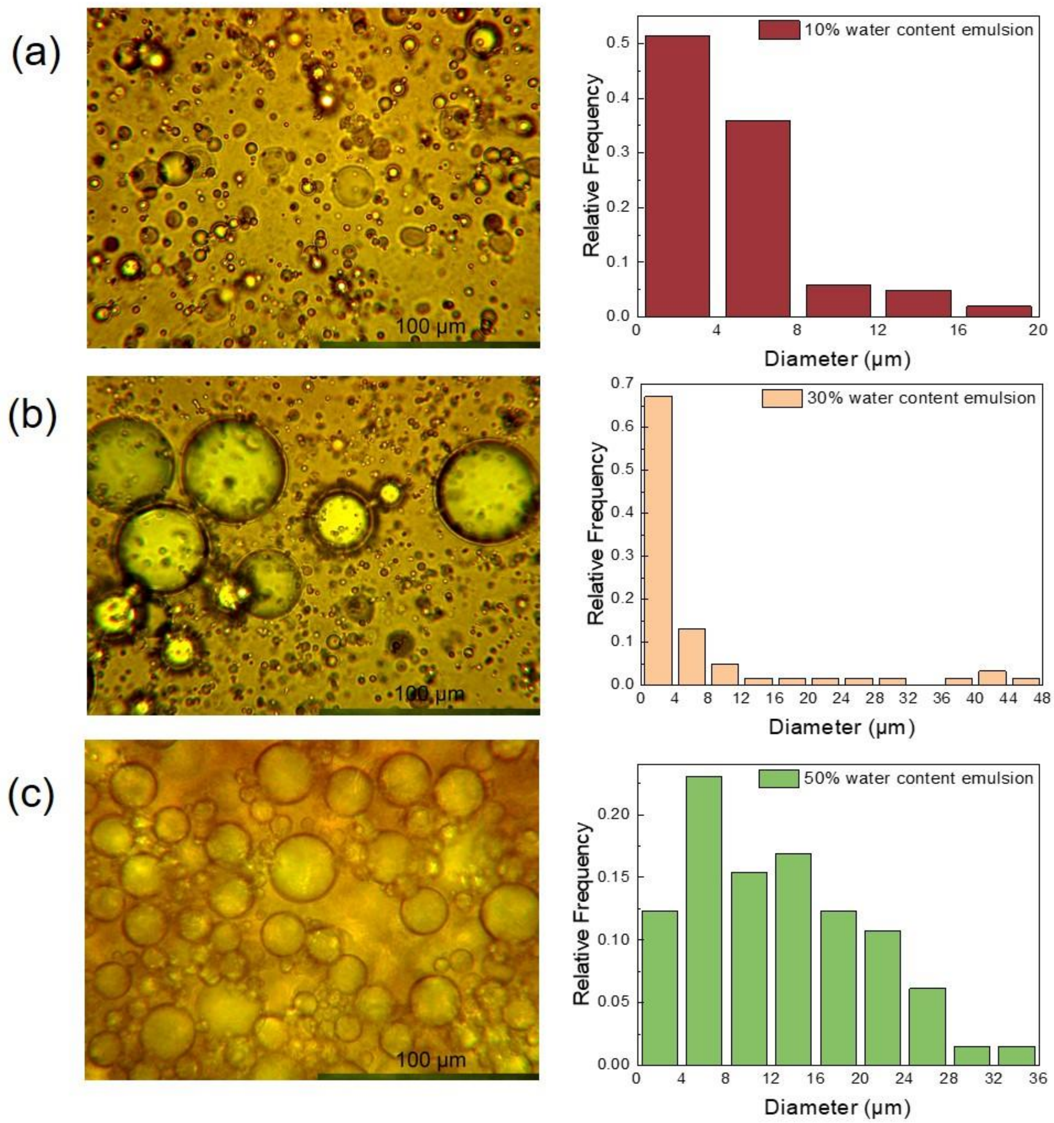

Figure 4-1. Microscopy and particle size distribution of emulsions with (a) 10% water content (b) 30% water content (c) 50% water content

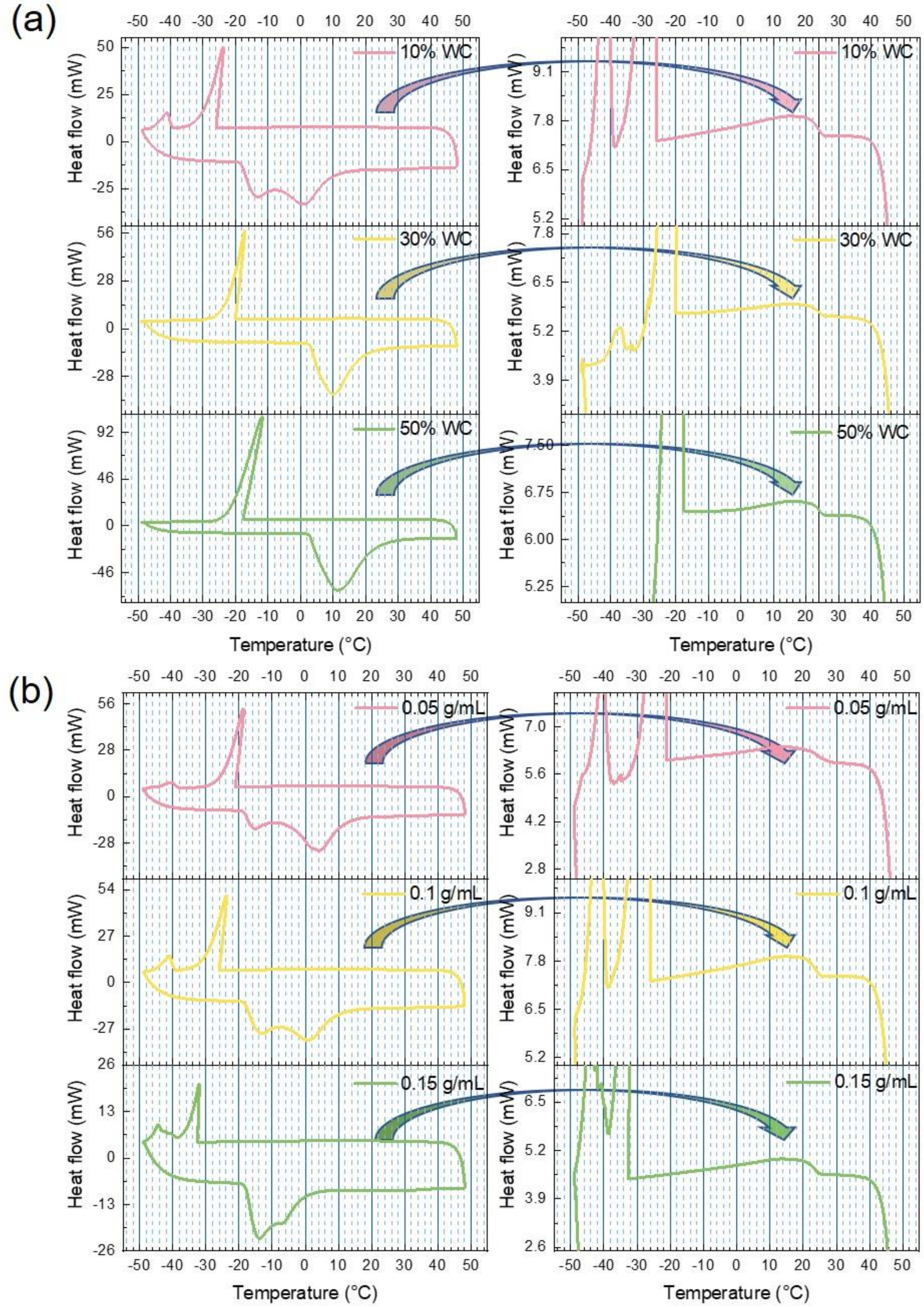

Figure 4-2. DSC images of emulsions with (a) different water content (b) 30% water content with different salinity level

DSC was used to record the thermal behavior of emulsions by detecting endothermic and exothermic processes. In Figure 4-2, the global DSC images are on the left and the partial magnified images are on the right. The left shows two significant peaks, one upright for water freezing and another upside down for ice melting. Normally, when the water droplets in emulsions freeze, the flow behavior is affected greatly. An increase in the salinity and a decrease in the water content of emulsions can significantly decrease the freezing temperature of the water droplets in W/O emulsions. However, in this experiment, crude oil reached its pour point (the temperature at which the crude oil loses its flow ability) above 0 ℃, so this freezing phenomenon did not exert any impact on the infiltration behavior. However, in the right magnified figure, there is another peak around 20 ℃, which stands for the wax appearance temperature (WAT). The method of determining the WAT of crude oil has been investigated in previous studies (Baltzer Hansen et al. 1991, Jiang et al. 2001, Kök et al. 2018). The appearance of paraffin wax would have a significant effect on the improvement of crude oil viscosity, thereby affecting the mobility behavior of spilled oil and emulsions. Nevertheless, the change in water content and salinity level played a negligible role in the WAT. Therefore, in this experiment, 5 ℃, 15 ℃, 23 ℃, and 30 ℃ were selected as target temperatures for all infiltration experiments to investigate the impact of temperature changes, the appearance of wax, and the pour point on the oil and emulsion infiltration.

The viscosity of emulsions with different water cuts under various temperatures and their fitting curves are presented in Figure 4-3. It is clear from the figure that the viscosity increased significantly with the increase in water content and the decrease in temperature. Furthermore, for all water contents, there are two different viscosity improvement phases. Above 20 ℃, the increasing slope is gentle and slow, whereas it is sharp and steep below 20 ℃. This is because of the precipitation of paraffin wax, which is consistent with the DSC results. Similar results were also found in other studies (Japper-Jaafar et al. 2016, Pedersen and Rønningsen 2003). The fitting curves can be used to calculate the viscosity at different temperatures and substituted into the model to simulate the infiltration process.

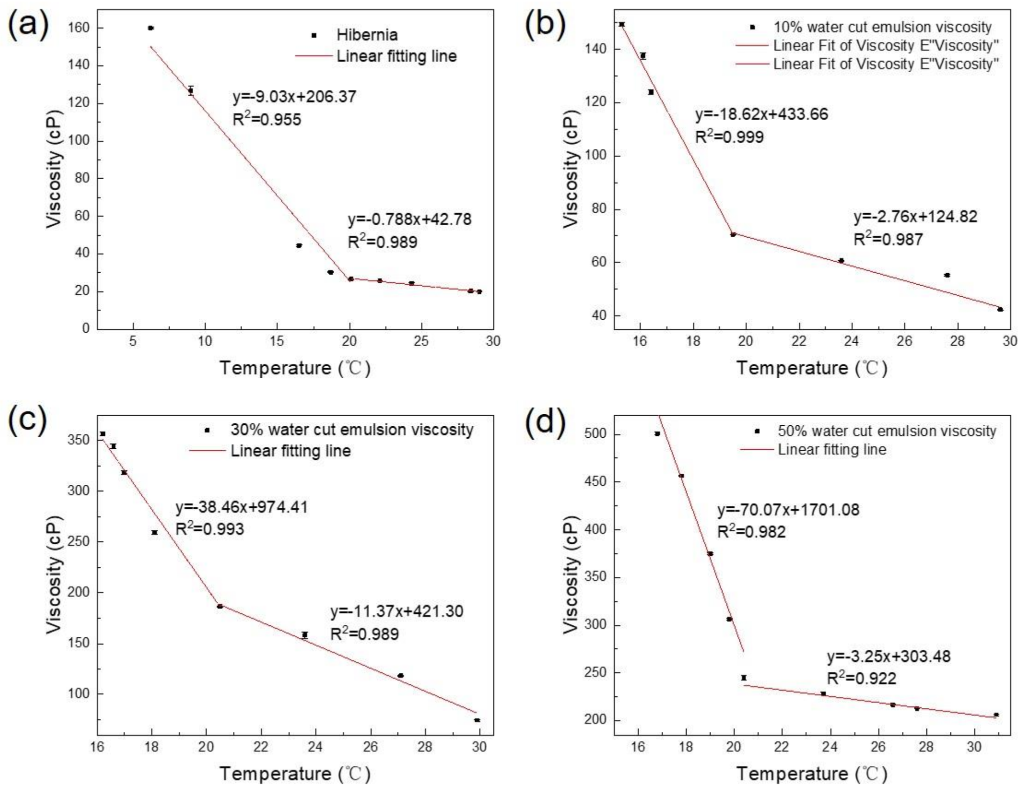

Figure 4-3. Viscosity at different temperatures of emulsions with (a) 0% water content (b) 10% water content (c) 30% water content (d) 50% water content

4.3.2. Effect of temperature and water cut on infiltration

The depth-time infiltration results of emulsions with different water cuts under various temperatures are presented in Figure 4-4. The results show that with the decrease in temperature, the infiltration rates, which could be considered the slope of the depth-time curve in the figure, reduced significantly for all water cuts from almost vertical curves at 30 °C to the situation where the emulsion nearly did not infiltrate at all at 5 °C. Obviously, the viscosity of oil or emulsions dropped sensitively with the temperature decrease, as shown in Figure 4-3 and reported in the literature (Qu et al. 2022). The soil used in this experiment was totally dry, indicating the condition of the soil medium was not changed. Another important reason is that in crude oil, a special chemical component is labelled paraffin, which consists primarily of long chain and saturated hydrocarbons from C_{18} to C_{75} normally and easily precipitates from crude oil at a certain temperature known as the

WAT or cloud point (Bhat and Mehrotra 2004, Kök et al. 2018). The DSC results in Figure 2 present an obvious peak between 20 ℃ and 30 ℃, illustrating the phase transformation from liquid to solid. The appearance of paraffin wax increases the system viscosity and reduces the infiltration velocity (Kruka et al. 1995). Therefore, when spill accidents happen, a high temperature will normally lead to more severe contamination.

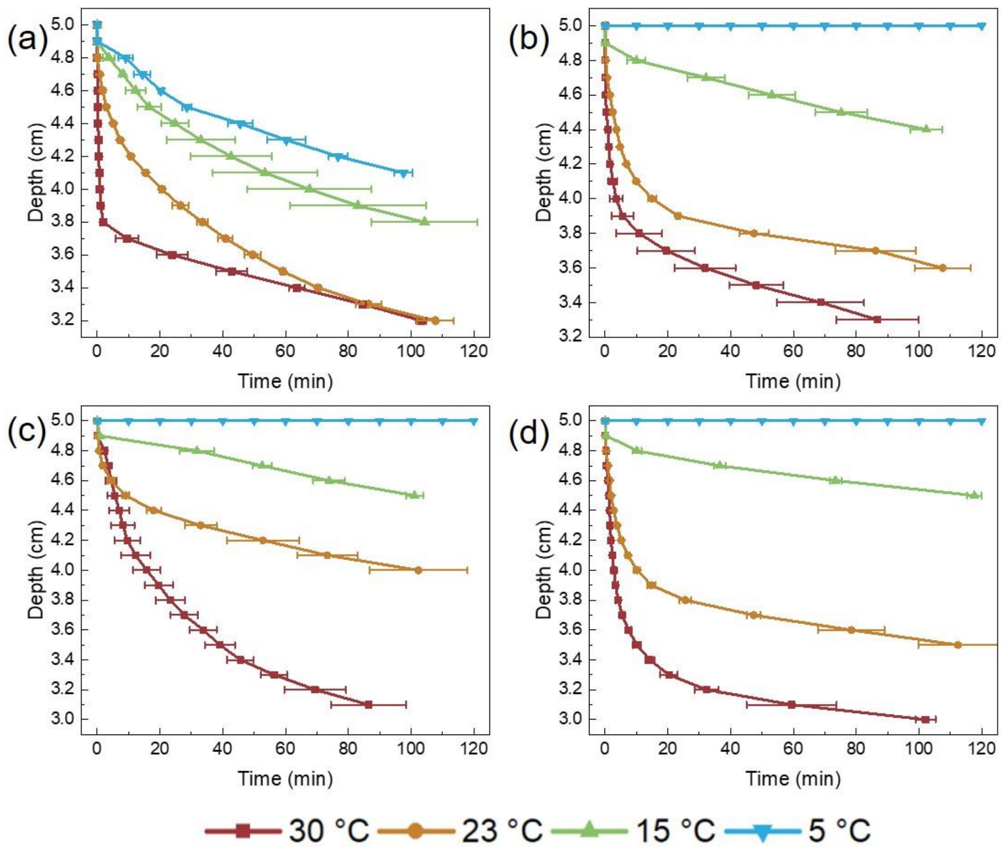

Figure 4-4. Infiltration curves at different temperature of emulsions with (a) 0% water content (b) 10% water content (c) 30% water content (d) 50% water content

Furthermore, for emulsions with different water cuts, when the temperature is as low as 5 ℃, emulsions transform from the liquid phase to the solid or semi-solid phase. Under this state, the W/O emulsion is so viscous that it cannot infiltrate at all. Figure 4-4 shows that Hibernia crude oil with 0% water content still had fluidity at 5 ℃ and infiltrated at approximately half the depth as it did at 30 ℃. However, as for emulsions with 10%, 30%, and 50% water content, they were too viscous to flow into the soil at 5 ℃, meaning they reached their pour point at this temperature. The reason that crude oil loses mobility is that paraffin crystals grow continuously below the WAT, resulting in a crystalline net to trap the liquid hydrocarbon molecules until the oil cannot flow (Taraneh et al. 2008). The pour point of the Hibernia blend crude oil according to an Exxon Mobile report is 37.4 °F, which is 3 °C (John Jechura 2018), so Hibernia crude oil did not lose fluidity as expected. Nevertheless, the water in the Hibernia crude oil emulsion losing mobility means the water content improved the pour point of emulsions above 5 °C. In a previous study, Visintin et al. (2008) reported that the presence of water changed the pour point temperature of a waxy crude oil emulsion gel because the wax crystals coated the surface of the liquid (reducing its tendency to coalesce) and impeded the free movement of the droplets within the emulsion. Hence, when oil spills occur, the formation of water in an oil emulsion may help hinder the infiltration of spilled oil and reduce pollution to the soil environment.

Another observed phenomenon is the infiltration of emulsions with a 50% water cut. It was reported that increasing the water content in an emulsion system could lead to the enhanced viscosity of the emulsion system (Abdulredha et al. 2020). Based on such consideration, a 50% water content emulsion should be the most viscous and have the slowest infiltration compared with Hibernia crude oil and 10% and 30% water content emulsions. However, as shown in Figure 4-4, the fastest infiltration curve is that of the 50% water cut emulsion at 30 °C and 23 °C. At 30 °C, within the same time period, the emulsion with a 50% water cut reached the deepest soil layer. Within the first 10 min, the emulsion arrived at approximately 3.5 cm, whereas the others reached 3.5 cm in about 30 to 40 min. When the temperature was 23 °C, although the 50% water cut emulsion did not show the deepest infiltration, the infiltration rate was still quite fast, almost the same as that of the emulsion with 10% water content. However, at 15 °C, it became the slowest, as expected, and it changed to a semi-solid gel at 5 °C, not infiltrating at all. The 50% water content emulsion experienced demulsification while infiltrating into the soil. The first reason is that an emulsion with a high water-content, such as 50%, is unstable compared with emulsions with 10% and 30% water content (Kilpatrick 2012, Pang et al. 2021, Wong et al. 2015). Under the same conditions, the stability is worse, and the stable time is shorter for 50% water content emulsions. Moreover, by combining the oil concentration distributions depicted in Figure 5, it was observed that the emulsion with a water content of 50% infiltrated the fastest at 30 ℃. The disparity in oil concentration between the top layer (1693.73 mg/L) and the bottom layer (577.33 mg/L) at 30 ℃ was nearly three times, much larger compared to the disparities observed in other emulsions, which were only about 1.5 to 2 times. This means that only an extremely small amount of oil reached the bottom soil layer. Thus, assuming the liquid that reaches the bottom is mainly water is reasonable. Furthermore, some researchers have concluded that a hydrophilic polymer membrane is a useful and effective tool to demulsify emulsions, whether water-in-oil or oil-in-water, by separating the water phase and the oil phase (Panatdasirisuk et al. 2017). Due to the fact that the dry soil used in this experiment is highly hydrophilic, it is likely to adsorb water droplets and demulsify an unstable emulsion with a 50% water cut. Hence, for the above reasons, it is assumed that a 50% water content emulsion demulsifies during the infiltration process. As for the slow infiltration rate of an emulsion with 50% water content at 15 ℃, it is because the decrease in temperature results in the precipitation of paraffin wax, forming a crystalline net to trap the water and liquid hydrocarbon molecules, causing the viscous movement of the emulsion system (Paso et al. 2009, Taraneh et al. 2008, Visintin et al. 2008).

It is concluded from this part that a decrease in temperature and an increase in water cut reduce the infiltration depth and rate of emulsion due to the improvement of viscosity and the appearance of solid paraffin wax until the emulsion system reaches the pour point and does not infiltrate at all. However, an overly high water cut causes low stability and demulsification of an emulsion, further leading to accelerated infiltration process, whereas a low temperature and paraffin wax would reduce this impact. Consequently, when spill accidents occur, response work needs to be more targeted. Properties such as the pour point, water content, paraffin content, and viscosity, as well as local temperature, are priorities to acquire.

4.3.3. Oil concentration of different soil layers during infiltration

The results of residual oil concentration after infiltration are presented in Figure 4-5. It is shown that the decrease in water content substantially resulted in the oil being concentrated in every soil layer at every ambient temperature. The volume of spilled liquid poured into the soil was 1 mL, which was the same for different conditions. Thus, higher water content means less oil content, leading to less severe contamination. Furthermore, it is noticed that for all levels of water content, oil tends to stay at the top layer at lower temperatures. The largest ratio of concentration at the top layer and bottom layer was observed at 5 ℃ or 15 ℃, whereas the concentration distribution at 23 ℃ and 30 ℃ tended to be even and homogenous. The highest concentration at 5 ℃ or 15 ℃ was always at the top layer, whereas for 23 ℃ and 30 ℃, it could be in the middle layer of soil, such as for 10% water content, where the concentrations at the 4.6 cm and 4.2 cm layers were greater than at the 5 cm layer. Similar results were also reported in our previous study that for soils with low porosity, low temperature, and high water content, more oil could be retained in the higher soil layer; in soils with high temperature, low water content, and high porosity, most of the oil was trapped in the deeper soil layers (Qu et al. 2022). This could be due to the reduction in the emulsion's viscosity. Figure 4-3 shows that the viscosity reduced when the temperature decreased, which made the infiltration rate of the emulsion decrease so greatly that most of the emulsion stayed at the top soil layer and only flowed down a little.

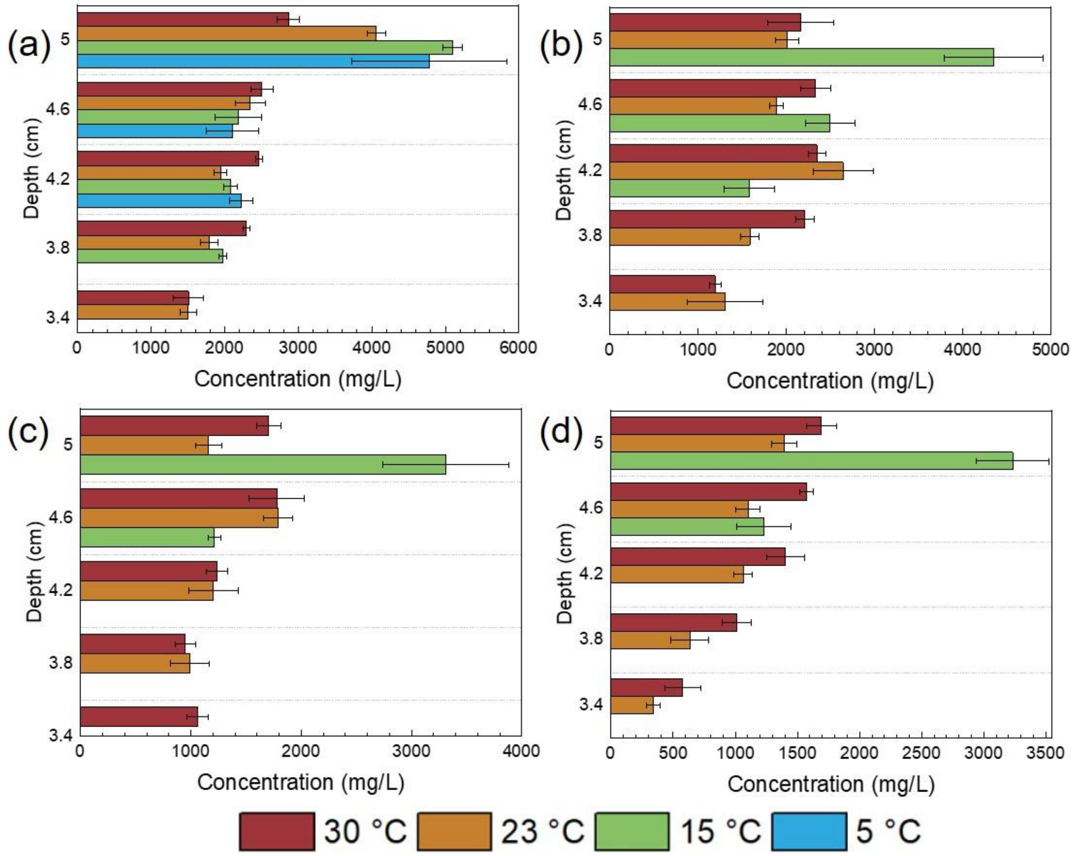

Figure 4-5. Oil concentration in different soil layers at different temperatures of emulsions with (a) 0% water content (b) 10% water content (c) 30% water content (d) 50% water

Furthermore, there was an interesting pattern for the concentration of 50% water content. At 23 ℃ and 30 ℃, the ratio of concentration at the top layer and bottom layer of the 50% water cut was still larger than that of other water cut emulsion. As discussed above, this was because of the instability and demulsification of the 50% water content emulsion. Finally, there were no concentration data for 10%, 30%, and 50% water cut emulsions at 5 ℃ since the increase in water cut caused the pour point to improve so that the emulsion became a gel and semi-solid at 5 ℃ and did not infiltrate at all. Thus, the concentration was 0.

According to the concentration results, at a low temperature, spilled oil tends to remain on the top layer of soil; at a high temperature, oil is likely to infiltrate into deeper layers. The distribution is relatively even and uniform at different soil layers. A high water content emulsion could demulsify during the infiltration process. Consequently, when oil or W/O emulsion spills occur, emergent responses must be adjusted according to the local conditions at the moment. If it is summer or the weather is warm, the soil of all polluted layers would be under severe threat and must be remediated; if it is winter or the weather is cold or the spilled liquid contains a large amount of water, the top soil layer retains most of the oil and can be the remediation focus.

4.3.4. Effect of salinity level on emulsion infiltration

Salinity is an important factor of various environmental pollutions (Khadanga et al. 2022, Yuan et al. 2022).In the process of enhanced oil recovery and improved well productivity, a large amount of brine water is produced and emulsified with crude oil during waterflooding (Mohamed et al. 2018, Yao et al. 2022). Many studies have shown that the salinity of aqueous water droplets in oil emulsions has a significant effect on the droplet size and emulsion stability (Al-Yaari et al. 2015, Maaref et al. 2017, Moradi et al. 2011). Thus, the impact of different salinity levels on emulsion infiltration was investigated in this part.

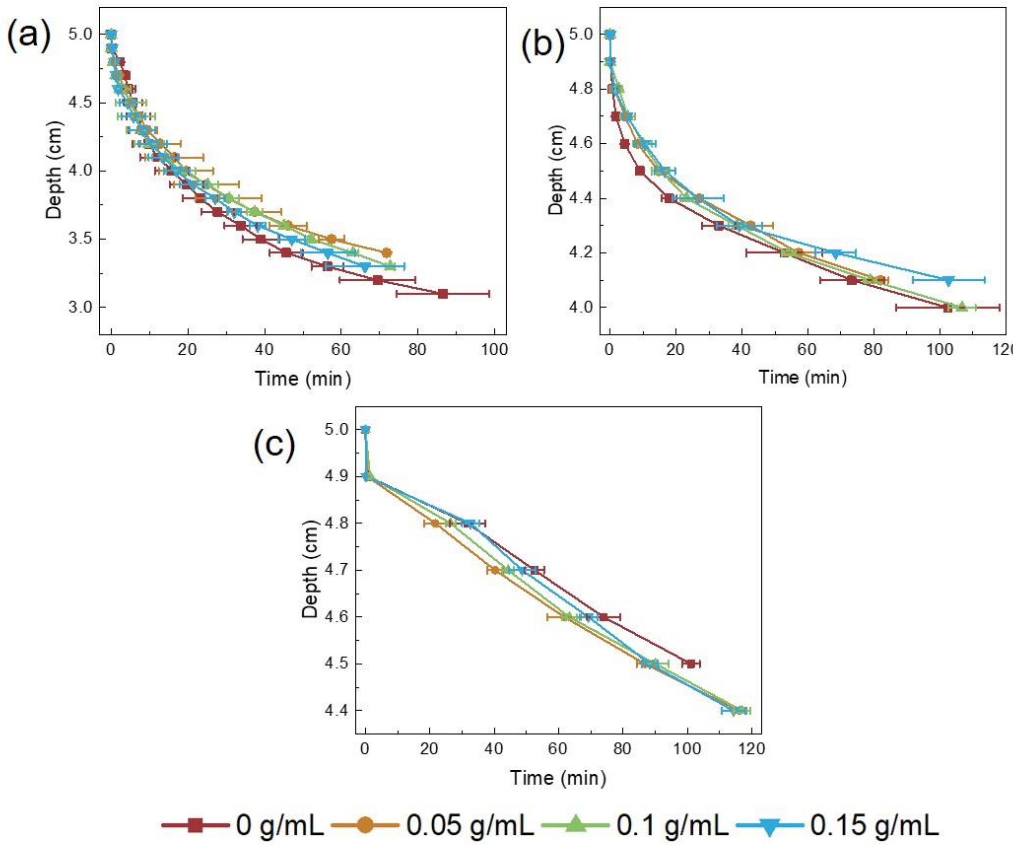

Figure 4-6. Infiltration curves of 30% water content emulsion with different salinity levels at (a) 30 ℃ (b) 23 ℃ (c) 15 ℃

Figure 4-6 illustrates that at three different temperatures, four emulsions with different salinity levels did not show obvious differences in their infiltration curve. According to Figure 4-2, although the water freezing temperature reduced significantly with the increase in salt content, the WAT remained the same for different salinity levels at about 24 ℃. This result is similar to that reported in the article of Maaref et al. (2017) who conducted a rheology experiment of brine water in crude oil emulsions using a glass etching micromodel, and found that the emulsion viscosity and interfacial tension increased slightly with salinity but did not significantly affect the flow behavior . Therefore, the salinity level did not exhibit a significant impact on the emulsion infiltration in this experiment. However, if there is no pour point for spilled oil, or the flowability disappearing temperature of oil is far lower than 0 ℃, the situation will be completely different. Due to the supercooling effect, the water freezing temperature was about −20 °C for the emulsion with a 30% water cut without added salt. However, this temperature decreased to −32 °C with the increase in salt content. Consequently, the flow behavior would be much different at the same temperature for various brines in oil emulsions, not to mention the impact brought by the difference in the freezing points of water and oil. Therefore, when a spill happens, the salinity level of water droplets in the W/O emulsion will have a negligible effect on the infiltration behavior of the oil for which the pour point is above 0 °C. Nevertheless, as for oil with a pour point or freezing point far lower than 0 °C, the flow pattern is still not clear, and more research needs to be conducted to investigate the mechanism and infiltration principle of this situation.

4.3.5. Impact of solid particles on infiltration behavior

Fine particles stabilizing W/O emulsions are frequently seen in oil extraction wells, oil recovery operations and heavy oil thermal recovery from tar bars (Levine et al. 1989, Menon and Wasan 1988). Thus, the impact of fine particles on emulsion infiltration was also studied in this study. According to previous research, fine particles have an imperative impact on emulsion stabilization (Levine et al. 1989). The ability of fine particles to constitute a tight and consistent film makes them an influential stabilizing agent, and the wettability of fine particles plays a significant role in the type of emulsion that forms (Menon and Wasan 1988, Yan et al. 2001). Moreover, it was also reported that the presence of fine particles improved the viscosity of an emulsion system and some models have been developed to quantify this change (Shi et al. 2018). Therefore, based on the common existence, crucial impact on emulsion stabilization, and apparent effect on the infiltration process, the surface-modified montmorillonite clay was used in this experiment to investigate the influence of fine particles on emulsion infiltration.

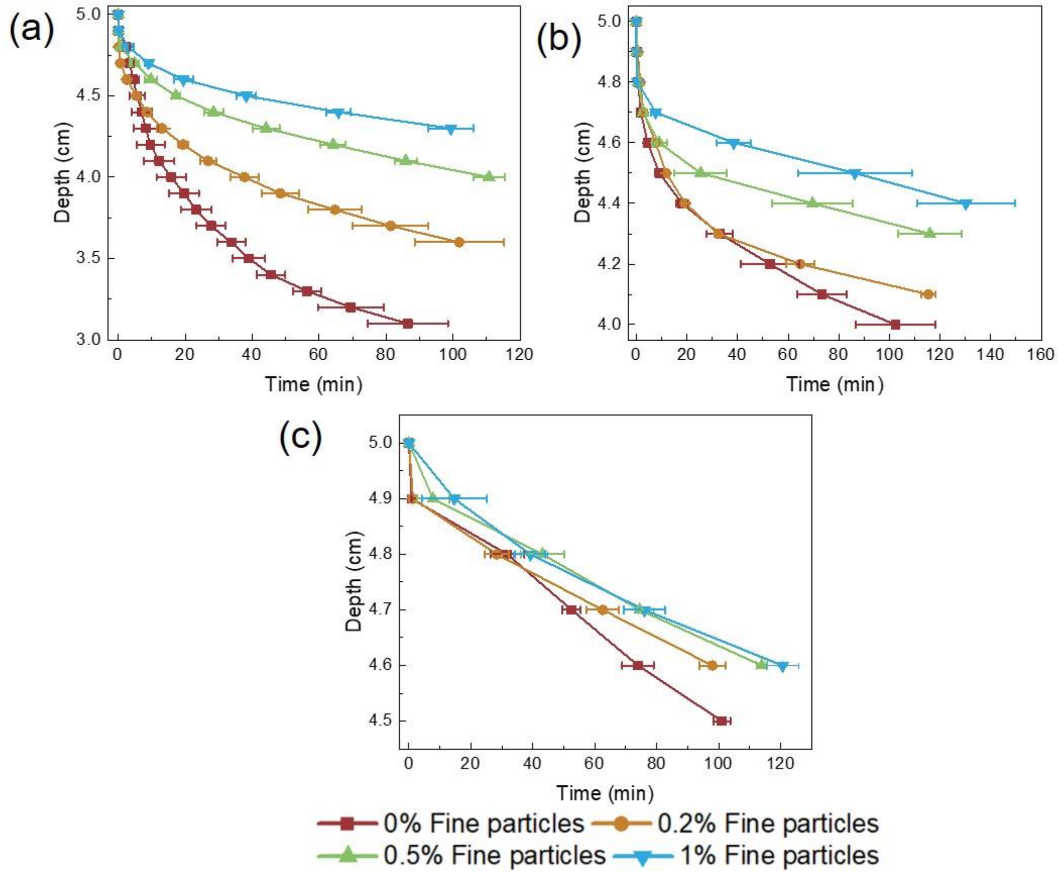

Figure 4-7. Infiltration curves of 30% water content emulsion with different fine particle levels at (a) 30 ℃ (b) 23 ℃ (c) 15 ℃

Figure 4-7 shows that at 30 ℃ and 23 ℃, the infiltration rate decreased with the increase in particle amount. The infiltration behavior of the emulsion with 1% fine particles at 30 ℃ was similar to that of the emulsion without fine particles at 15 ℃, reaching about 4.5 cm in 100 min, which is an obvious impediment to emulsion flow. One reason for this hindrance impact is the viscosity improvement due to the presence of fine particles. Another important cause, we believe, is the filter impact of soil layers on fine particles, resulting in a decrease in porosity, which leads to clogging and a reduction in the infiltration rate (Qu et al. 2022). Using sand medium to filter water and treat drinking water has been studied extensively (Freitas et al. 2022, Napotnik et al. 2017, Song et al. 2020b). Sand layers with a particle size of approximately 150 mm, similar to the soil particles used in this experiment, can filter and remove the fine particles in drinking water efficiently via attraction force and close-range molecular forces such as van der Waals forces. Consequently, for the above two reasons, it is reasonable to explain the obstruction effect of fine particles in emulsion systems on infiltration processes. However, in the 15 ℃ situation, four emulsion systems with various fine particle numbers had similar infiltration curves. This means when the temperature decreases and the wax crystalline structure grows, the wax is the dominant factor in the viscosity and flow pattern. The infiltration curves of 10%, 30%, and 50% water cut emulsions in the preceding section about temperature and water cut impact also confirm this conclusion. After the spill incident, an emulsion with large numbers of fine particles will infiltrate at a slow rate even at a high temperature due to the high viscosity and clogging impact. At a low temperature, similar infiltration patterns for emulsions with the same water cut would be observed.

4.3.6. Simulation of emulsion infiltration processes

Modeling has been widely used to analyze the various environmental processes (Feng et al. 2020, Valikhan Anaraki et al. 2022, Yadav et al. 2022). Currently, there are mainly two different methods to describe emulsion infiltration behavior. One is to consider the W/O emulsion as two different phases that interact with each other and porous media independently. These methods focus on the relationship between the droplet size of the emulsion and the pore size of porous media to investigate the blocking effect of emulsion droplets on the throat of porous media and permeability changing. However, such method was mainly about W/O emulsions (Soo and Radke 1986, Spaid and Phelan Jr 1997). Another method to describe the emulsion infiltration is to regard the emulsion as a continuum and single-phase fluid with no permeability changes but only viscosity (Savins 1969). Considering the practicality, the latter method was selected in this study. Figure 4-8 was obtained by solving the Green-Ampt formula in section 3.2.3. The variable in the formula is the conductivity K. According to equation (iii), letting D equal 0.1 mm causes the soil particle size to increase from 0.106 mm to 0.205 mm, and K is calculated as 0.00648 cm/s. In a real oil spill response, K could be obtained via either the conductivity measurement experiment or particle size measurement depending on which is more convenient. Therefore, the viscosity of the emulsion would be K * $(\rho_{oil}/\rho_{water})$ *

($\mu_{water}/\mu_{emulsion}$). Different conditions were controlled by the parameter $\mu_{emulsion}$, which is related to the ambient temperature and the water cut of emulsions.

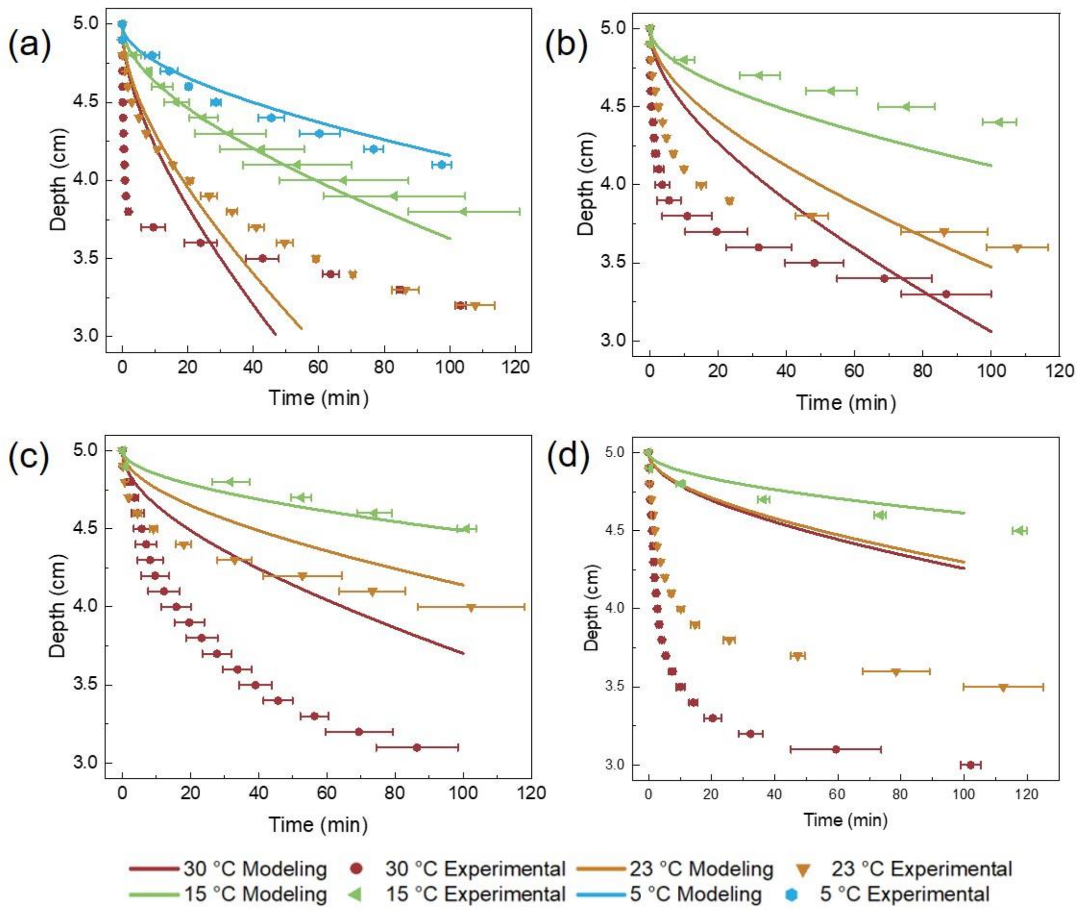

Figure 4-8. Infiltration data and simulating curves at different temperatures of emulsions with (a) 0% water content (b) 10% water content (c) 30% water content (d) 50% water content

From Figure 4-8, it is apparent that the Green-Ampt model is more suitable for high-viscosity emulsions and low-speed infiltration situations. Hibernia crude oil at 5 °C and 15 °C and emulsions at 15 °C were all simulated well with the model. However, as for the high-temperature and low-viscosity situation, the simulation was unsatisfying. The simulation infiltration was too slow at the beginning but too fast at the end under the situations of Hibernia and 10% and 30% water cut emulsions at 23 °C and 30 °C. These phenomena may be caused by the assumption of the Green-Ampt model, which is derived from Darcy's law. The pressure head gradient was replaced by the liquid height and infiltration head, sometimes with the capillary head. Consequently, according to this hypothesis, the flow controlled by the Green-Ampt model would never stop (Hilpert and Glantz 2013). However, the pressure head caused by the infiltrated liquid was not equal to the infiltration depth due to the existence of adhesive force between soil particles and the infiltrating liquid. The pressure head would increase to its maximum value with the infiltration and decrease to zero gradually when it reached the final layer because the soil matrix suction is highly related to its liquid content (Sreedeep and Singh 2011, Yang et al. 2004). Furthermore, due to the fact that the capillary head was ignored and there was conductivity difference between dry soil and saturated soil which is assumed in Darcy's law (Kale and Sahoo 2011, Klute 1952), the slower simulated infiltration at the beginning was also reasonable (Kale and Sahoo 2011). As for the 50% water content emulsion, because of the demulsification, which was explained above, the simulation was significantly different. Hence, the modification of capillary pressure and infiltrated liquid pressure and the conductivity difference between real soil and saturated soil are the main reasons for the difference between the modeling and experimental data. Nevertheless, due to the simplicity and practicality of the Green-Ampt model, it could still be used to predict infiltration, especially under the situation of low temperature and high viscosity.

4.4. Summary

This study investigated the infiltration of spilled W/O emulsion into soil and the related influencing factors. The results showed that an increase in the water content of an emulsion and the existence of fine particles would improve the viscosity of the emulsion, thereby decreasing the infiltration depth. This phenomenon could also be affected by a reduction in temperature, which results in the precipitation of paraffin wax when the temperature reaches the WAT, exacerbating the enhancement of viscosity and reduction of infiltration depth. However, excessive water content at a high temperature could cause demulsification, leading to a much deeper infiltration. Although the salinity level exerted an important impact on the freezing temperature of water droplets in the emulsions, it did not show a distinct impact on the infiltration process considering that Hibernia crude oil and its W/O emulsions reached their pour point before freezing. The adopted Green-

Ampt model showed a good simulation performance when the temperature was low. The concentration distribution of oil was also studied, and a conclusion was drawn that the spilled oil tends to remain on the top layer of soil at a low temperature and is likely to infiltrate into deep layers with a relatively even and uniform distribution in different soil layers at a high temperature. The results of this study can help better understand the behaviors of spilled emulsions and develop the corresponding response strategies.

CHAPTER 5. THE IMPACT OF PLANT ROOTS ON THE INFILTRATION PROCESS IN INLAND OIL SPILL ACCIDENTS

5.1. Background

Inland oil spills are major disaster for ecological system and human beings and arise great concerns in the public. When inland spills occur, one of the most common behaviors of spilled oil is infiltration into soil. If the emergent response cannot be taken in time, spilled oil would infiltrate into deep soil layer and even reach the groundwater, causing great contamination to the drinking water supply system (Huang et al. 2017). Therefore, the infiltration process of spilled oil into soil environment needs to be well researched to reduce the contamination and risks brought from inland oil spill accidents.

Several prior studies have been undertaken to examine the infiltration behavior of both aqueous and non-aqueous liquids into soil and other porous media. As an example, McCauley et al. (2002b) conducted a study in which they compared the hydraulic conductivities and infiltration rates of fuels in frozen and unfrozen soils. Their observations indicated that higher ice content resulted in a notable decrease in hydraulic conductivity and infiltration rates. Among various soil types, sandy silty soil with smaller particle sizes exhibited the lowest hydraulic conductivity and infiltration rate, in contrast to soils with larger particle sizes. Our previous experiments also investigated the impact of thawing frozen soil and formation of water in oil emulsions on the infiltration process (Qu et al. 2022, Qu et al. 2023). Moreover, some papers studied the impact of plant roots on the water infiltration to soil and revealed that the infiltration process were governed by complex interactions between the plant and soil components (Hangen et al. 2002, Liu et al. 2019, Meek et al. 1992). However, the impact of plant roots has never been investigated which is very common in the nature.

Therefore, in this experiment, (1) the impact of plant roots and nettings on the infiltration rate and depth of spilled oil will be studied; (2) residue concentrations in different soil layers will be investigated. Hopefully, this research could give some basic help to the emergent response of inland oil spills.

5.2. Materials and methods

5.2.1. Materials

The samples were dried and sieved using 600-μm, 1-mm and 2-mm sieves. Particle density was measured using the pycnometer method. Engine oil (15W-40) from the Shell company was used as a representative oil The basic information of oil and soil properties is listed in Table 5-1. Analysis-grade n-heptane were purchased from Fisher Chemical. Deionized water was used in all experiments.

5.2.2. Experiment procedures

This research encompassed two experiments aimed at investigating the impact of plant roots. To explore the impact of plant roots, two different nettings were employed to simulate the plant roots, each with varying mesh sizes. The first netting had a mesh size of 2845 (441 holes per 1 cm^2) while the second netting had a mesh size of 58 (9 holes per 1 cm^2). Both nettings were constructed using Nylon material. A soil sample (5 cm) was introduced into a plastic column with a 13.5-mm inner diameter, which was ventilated at the bottom to replicate a real soil environment. After placing the nettings at different soil layers, a rapid pour of 1.0 mL of engine oil onto the top of soil initiated the filming process to record the ensuing process.

Following the completion of the infiltration experiments, soil samples were excavated at 0.4 cm intervals, and 0.1 g of each 0.4 cm interval's soil column was transferred to individual 20-mL glass vials. The oil extraction and concentration test method was as same as that in Chapter 4.

The netting experiments were conducted under following conditions: two soil particle ranges (0.6-1 mm and 1-2 mm); four distinct nettings (no netting, 1 netting with a mesh size of 58, 1 netting with a mesh size of 2845, and 3 nettings in row with a mesh size of 2845); and three soil layers (5 cm, 4.5 cm, and 4 cm). All experiments were conducted in room temperature (23 °C).

5.3. Results and discussion

5.3.1. Effect of nettings with various mesh sizes on infiltration

The depth-time results of oil infiltration in various soils with nettings with different mesh sizes at various heights are presented in Figure 5-1. From the figure, it is evident that the 1 and 3 fine nettings (mesh size of 2845) impeded the infiltration process of oil significantly. However, the coarse netting (mesh size of 58) only showed a slight impact on the infiltration rate. For instance, in subfigure (b), the infiltration rates were similar above 4.5 cm. However, after passing the netting at 4.5cm, the infiltration rates in soil with 1 and 3 fine nettings were dropped rapidly, reaching 4.2 cm in over 1 minute, while the infiltration rate in soil with coarse netting still remained similar to that without netting, reaching 4.2 cm in about 0.75 minutes. All 6 subfigures exhibited similar impact of nettings except for subfigure (c). This difference was inconsequential simply because the oil stopped infiltrating in soil column with fine nettings at height of 4 cm. The reason for the influence of mesh size of netting lies in the pore and throat size of soil which affect soil permeability. Previous studies have demonstrated that the permeability of soil with varying particle sizes is significantly influenced by the number and volume distribution of pores and the permeability of soil increases with the increase in pore sizes (Fan et al. 2021, Steinwinder and Beckingham 2019). In this experiment, the mesh size of coarse netting is larger than the pore sizes while the mesh size of fine netting is smaller than the soil pore sizes. Consequently, the coarse netting did not show any obstruction to the infiltration process whereas the infiltration rates decreased with the using of fine nettings. This can be attributed to the pore size of the coarse netting being 3.3 mm, the fine netting being 0.5 mm, and the soil pore size being nearly 1:1 with the grain size, as evident in the corresponding pore size range discussed in the paper (Fan et al. 2021, Nelson 2009). Several papers have demonstrated that the presence of plant roots can enhance soil pore size, leading to improved water infiltrability in the soil (Liu et al. 2019, Wang et al. 2022a). However, this phenomenon did not occur in this experiment. Therefore, when spilled oil infiltrates and encounters plant roots in the soil, the infiltration process would not be significantly affected if the plant roots are sparse. However, if the plant roots are dense with an intensive network of root hairs, the infiltration process may be hindered.

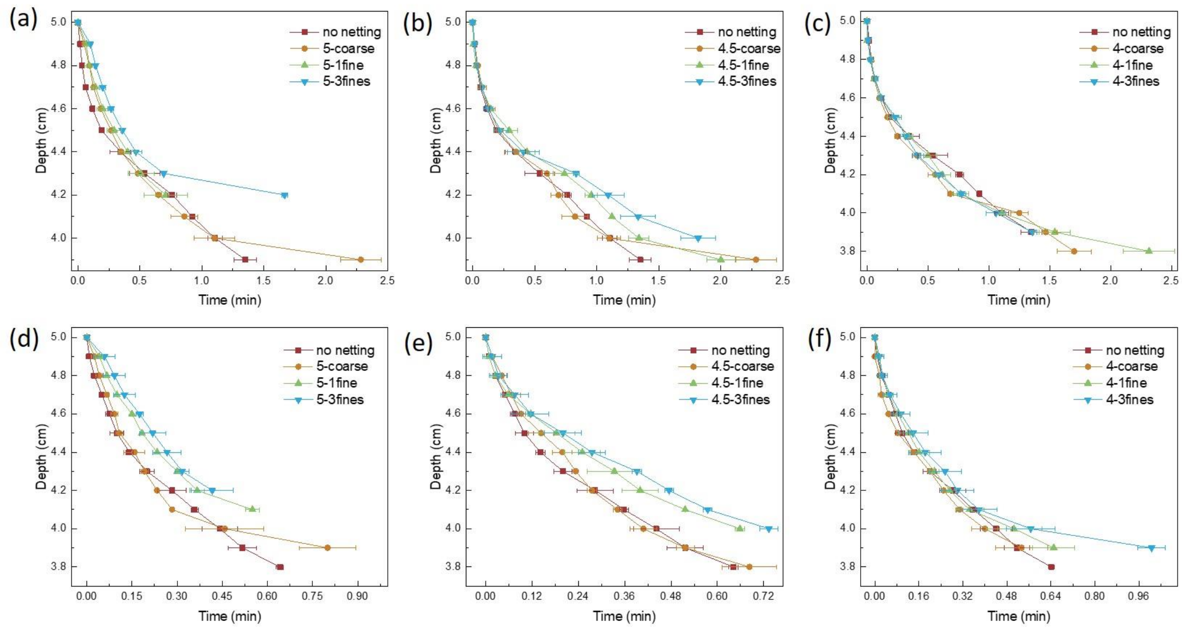

Figure 5-1. Infiltration curves of oil in (a) 0.6-1 mm soil with nettings of various mesh sizes at 5 cm height (b) 0.6-1 mm soil with nettings of various mesh sizes at 4.5 cm height (c) 0.6-1 mm soil with nettings of various mesh sizes at 4 cm height (d) 1-2 mm soil with nettings of various mesh sizes at 5 cm height (e) 1-2 mm soil with nettings of various mesh sizes at 4.5 cm height (f) 1-2 mm soil with nettings of various mesh sizes at 4 cm height

Besides, it is shown from Figure 1 that the position of netting plays an obvious role in the infiltration process. The changes of infiltration rate always started at the height of netting. For example, in subfigure (a) and (d), the distinction is apparent right from the beginning and in subfigure (b) and (e), the difference becomes evident at around 4.5 cm. The same pattern also applies to subfigure (c) and (f). Moreover, the presence of fine nettings at 5 cm depth also resulted in a decrease in the oil infiltration depth compared to nettings at other heights. For instance, in soil columns with three layers of fine netting, the oil infiltrated to a depth of 4.2 cm when the nettings were placed at 5 cm. However, when the nettings were positioned at 4.5 cm and 4.0 cm, the oil reached depths of 4.0 cm and 3.9 cm, respectively. For this reason, it is concluded that the obstruction effect is more significant when the netting and plant roots are positioned at a higher level in the soil.

Furthermore, the impact of mesh size of netting varies depending on the particle size ranges of the soil. When using nettings of the same mesh size, the obstruction effect is more noticeable in soil with particle sizes ranging from 1 to 2 mm compared to soil with particle sizes ranging from 0.6 to 1 mm. A compelling example can be observed in the infiltration of soil with nettings placed at a height of 5 cm (subfigures (a) and (d)). The difference in infiltration rates is significantly more pronounced among the curves in subfigure (a) compared to those in subfigure (d), particularly concerning the contrast between three fine nettings and no netting. Similar distinctions can also be observed in the other four subfigures. This phenomenon can be attributed to the differences in pore sizes of the respective soils, as mentioned above (Fan et al. 2021, Steinwinder and Beckingham 2019). The pore size in soil with particle sizes ranging from 1 to 2 mm is larger than that in soil with particle sizes ranging from 0.6 to 1 mm. Hence, when encountering fine nettings with same mesh size, the oil infiltration rates would decrease more in soil with a greater pore size. Therefore, the impact of nettings and plant roots on infiltration process is more significant in soil with large particle size ranges.

In summary, the results of this study indicate that the presence of nettings and plant roots has a considerable impact on the oil infiltration process in various soils. The nettings with a finer mesh size and denser plant roots show a more significant effect on the infiltration process, particularly when their pore size is smaller than that of the soil. The position of the nettings plays a crucial role in influencing the infiltration rate, consistently observed across all subfigures. A top and bottom position typically results in greater obstruction impact. Moreover, the obstruction effect is more pronounced in soils with larger particle size ranges, which can be attributed to the differences in pore sizes. This highlights the significance of nettings and plant roots in influencing infiltration processes under different soil conditions.

5.3.2. Oil concentration of different soil layers during infiltration

The oil concentration results in different soil layers are depicted in Figure 5-2. Notably, in certain cases, such as soil with 3 fine nettings at 5 cm, Figure 5-1 indicates the oil reaching only 4.2 cm. However, in Figure 5-2, traces of oil are still detected at a depth of 3.8 cm in the soil layer. This disparity can be attributed to the time-consuming process of excavating soil samples from each layer. During this period, the oil could further infiltrate, explaining why it is detected at a deeper level than the infiltration curves depicted in Figure 5-1. The unit "%" of concentration" refers to the oil percentage of specific soil layer in the soil column, used to compare the distribution differences under various conditions. From Figure 5-2, it is evident that the fine nettings have an obstructive effect on oil infiltration, as mentioned in section 3.1. The concentration of oil was higher in the soil layers above the nettings, and the bottom concentrations in the soil with fine nettings were significantly lower than in soil without nettings. For example, in the case of 0.6-1 mm soil with nettings at 5 cm (subfigure (a)), the concentration in the 5 cm soil layer with 3 fine nettings exceeds 30%, significantly higher than the concentration in the 5 cm soil layer without nettings, which is approximately 25%. Another compelling instance is observed in the soil with 3 fine nettings at 4 cm (subfigures (c) and (f)). The concentrations in the 4.2 cm layer of soil with 3 fine nettings are approximately 3% to 4% higher than that of the soil without nettings, whereas the concentrations in the 4.2 cm layer of soil with 3 fine nettings are 3% to 4% lower than that of the soil without nettings. However, in soil column with coarse nettings, the concentration distribution of oil is similar with that in soil without nettings. Based on these results, it is evident that nettings and plant roots can obstruct the forward infiltration of oil. Consequently, in the event of an oil spill accident, emergency response efforts should prioritize the areas above dense nettings and plant roots, where a higher concentration of oil tends to remain. If nettings and plant roots are not closely packed together, the emergency response could be treated similarly to the response for soil without nettings and plant roots.

Another intriguing discovery is that in soils with larger particle size ranges, the oil tended to accumulate in the bottom layer, while in soils with smaller particle size ranges, the oil preferred to remain in the top layer. This finding aligns with our previous study, where we observed that as the ice in the soil started to thaw and the porosity increased, the oil exhibited a tendency to accumulate in the bottom layer (Qu et al. 2022). Hence, in cases where the soil particles are small, the response work should primarily focus on the upper layer, as it is more susceptible to obstruction by soil. On the other hand, when the soil particles are large, the entire oil infiltration depth should be treated equally, as the obstruction effect from soil is less pronounced.

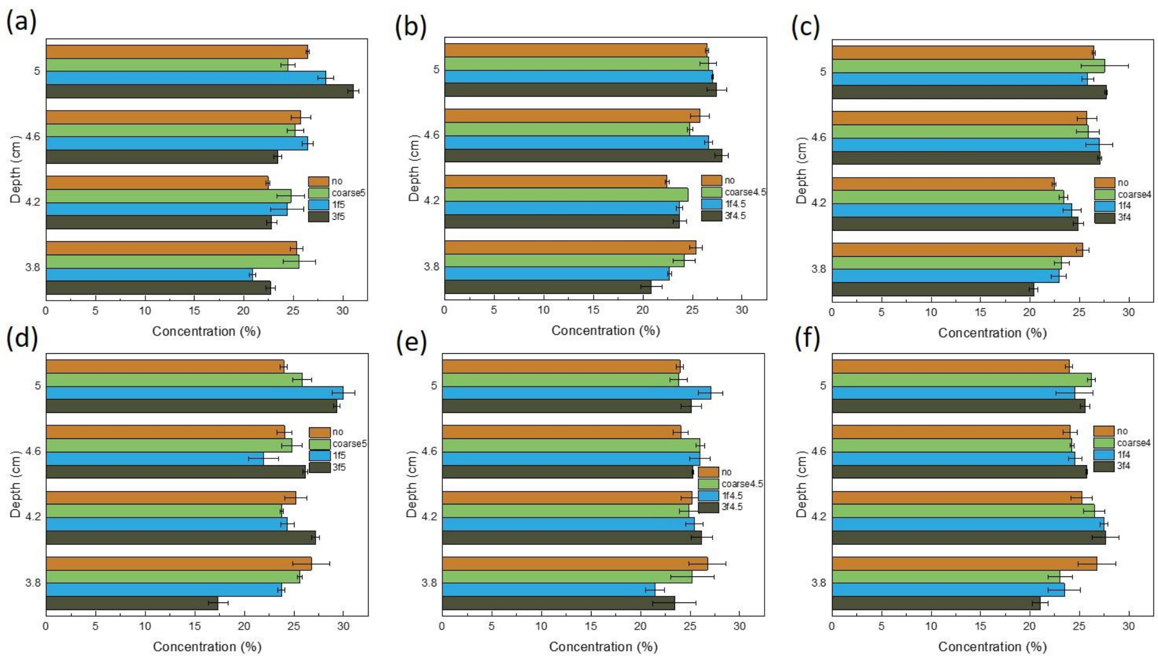

Figure 5-2. Oil concentration in different layers of (a) 0.6-1 mm soil with nettings of various mesh sizes at 5 cm height (b) 0.6-1 mm soil with nettings of various mesh sizes at 4.5 cm height (c) 0.6-1 mm soil with nettings of various mesh sizes at 4 cm height (d) 1-2 mm soil with nettings of various mesh sizes at 5 cm height (e) 1-2 mm soil with nettings of various mesh sizes at 4.5 cm height (f) 1-2 mm soil with nettings of various mesh sizes at 4 cm height

Furthermore, the positioning of nettings also affects the concentration distribution of oil. When the nettings were placed in the middle height of the soil column, the difference in oil concentration between soil with fine nettings and soil without nettings was slight. However, when the nettings were placed in the top layer or bottom layer of the soil column, the difference became significant. For instance, in subfigure (b) and (e), the concentration difference at 4.6 cm between soil with 3 fine nettings and soil without nettings was less than 2%. In contrast, in subfigure (a) and (d), or in subfigure (c) and (f), the concentration difference at 5 cm or at 4 cm between soil with 3 fine nettings and soil without nettings was greater than 5%. In actual inland oil spill accidents, the nettings and plant roots in the top and deeper soil layers can impede the infiltration of spilled oil, whereas the nettings and plant roots in the shallow or middle soil layers have a relatively minor obstructive effect on oil infiltration.

In conclusion, the positioning and density level of nettings and plant roots significantly impact the concentration distribution of oil. Higher oil concentrations are observed above soil layers with denser nettings and plant roots, particularly in the top and deeper soil layers. Additionally, in soils with larger particle size ranges, the oil tends to gather at the bottom layer, while in soils with smaller particle size ranges, it tends to stay in the top layer.

5.4. Summary

This study indicates that the presence of nettings and plant roots has a considerable impact on the oil infiltration process in various soils. The nettings with a finer mesh size and denser plant roots show a more significant effect on the infiltration process, particularly when their pore size is smaller than that of the soil. The position of the nettings plays a crucial role in influencing the infiltration rate. A higher position typically results in greater obstruction impact. Moreover, the obstruction effect is more pronounced in soils with larger particle size ranges, which can be attributed to the differences in pore sizes. Higher oil concentrations are observed above soil layers with denser nettings and plant roots, particularly in the top and deeper soil layers. Additionally, in soils with larger particle size ranges, the oil tends to gather at the bottom layer, while in soils with smaller particle size ranges, it tends to stay in the top layer. This study highlights the significance of nettings and plant roots in influencing infiltration processes under different soil conditions.

CHAPTER 6. CONCLUSIONS

6.1. Conclusions

In conclusion, this thesis research undertook a comprehensive exploration of the infiltration of spilled oil in soil under various environmental conditions. Through a thorough literature review and a series of focused studies, valuable insights were gained into the behavior, penetration, and distribution of spilled oil in different soil and weather conditions. The research revealed that factors such as temperature, water content, and soil type play pivotal roles in determining the infiltration patterns of spilled oil. The modified Green-Ampt model demonstrated effectiveness in simulating oil penetration, particularly in conditions characterized by low temperatures and high water-content. Additionally, the study highlighted the significance of external elements like netting and plant roots in influencing oil infiltration behavior and concentration distribution within soil layers.

These findings offer a deeper understanding of the complex interplay between oil spills and environmental factors, contributing to the formulation of more informed response strategies. The knowledge gained from this research serves as a valuable resource for enhancing emergency preparedness and effective mitigation measures in the event of inland oil spill incidents. As the world continues to grapple with the challenges posed by environmental contamination, this study provides a meaningful contribution to the ongoing efforts aimed at safeguarding our ecosystems and ensuring sustainable practices in the face of potential oil spill scenarios.

6.2. Recommendations for future research

(1) To enhance our understanding of inland spilled oil infiltration, it is expected to further conduct tests across diverse soil types, weather conditions, and spill scenarios. Real-world data will be used to refine insights into soil-oil interactions.

(2) 3-D simulation could be applied for detailed oil infiltration modeling. Simulation models can be further validated through experimental data to improve accuracy. Advanced simulations can provide insights into complex oil-soil dynamics.

(3) A predictive technique can be further developed for estimating oil infiltration depth and concentration in different soil layers, utilizing data from field tests and validated models. This tool will aid rapid assessment and targeted response strategies for inland oil spills, minimizing environmental and economic impact.

References

Abdulredha, M.M., Aslina, H.S. and Luqman, C.A. (2020) Overview on petroleum emulsions, formation, influence and demulsification treatment techniques. Arabian Journal of Chemistry 13(1), 3403-3428.

Afanas'ev, A. and Mel'nik, O. (2013) Mathematical modeling of multiphase seepage under near-critical conditions. Moscow University Mechanics Bulletin 68(3), 76-79.

Al-Yaari, M., Hussein, I., Al-Sarkhi, A., Abbad, M. and Chang, F. (2015) Effect of water salinity on surfactant-stabilized water–oil emulsions flow characteristics. Experimental Thermal Fluid Science 64, 54-61.

Amir-Heidari, P., Arneborg, L., Lindgren, J.F., Lindhe, A., Rosén, L., Raie, M., Axell, L. and Hassellöv, I.-M. (2019) A state-of-the-art model for spatial and stochastic oil spill risk assessment: A case study of oil spill from a shipwreck. Environment international 126, 309-320.

Amro, M.M., Benzagouta, M.S. and Karnanda, W. (2013) Investigation on crude oil penetration depth into soils. Arabian Journal of Geosciences 6(3), 873-880.

Andrade, R.B. (1971) The influence of bulk density on the hydraulic conductivity and water content-matric suction relation of two soils. Utah State University Thesis.

Aurell, J. and Gullett, B.K. (2010) Aerostat sampling of PCDD/PCDF emissions from the Gulf oil spill in situ burns. Environmental science & technology 44(24), 9431-9437.

Babamiri, O., Vanaei, A., Guo, X., Wu, P., Richter, A. and Ng, K. (2021) Numerical simulation of water quality and self-purification in a mountainous river using QUAL2KW. Journal of Environmental Informatics 37(1), 26-35.

Baltzer Hansen, A., Larsen, E., Batsberg Pedersen, W., Nielsen, A.B. and Roenningsen, H.P. (1991) Wax precipitation from North Sea crude oils. 3. Precipitation and dissolution of wax studied by differential scanning calorimetry. Energy & Fuels 5(6), 914-923.

Basit, A., KuShaari, K., Siwayanan, P. and Azeem, B. (2018) Effect of process parameters on droplet spreading behaviour over porous surface. The Canadian Journal of Chemical Engineering 96(1), 352-359.

Bhat, N.V. and Mehrotra, A.K. (2004) Measurement and prediction of the phase behavior of wax− solvent mixtures: Significance of the wax dis appearance temperature. Industrial Engineering Chemistry 43(13), 3451-3461.

Bhattacharyya, S., Klerks, P. and Nyman, J. (2003) Toxicity to freshwater organisms from oils and oil spill chemical treatments in laboratory microcosms. Environmental Pollution 122(2), 205-215.

Bi, H., An, C., Owens, E., Lee, K., Chen, Z., Mulligan, C., Taylor, E. and Boufadel, M. (2021) A framework for the evaluation and selection of shoreline surface washing agents in oil spill response. Journal of Environmental Management 287, 112346.

Bragg, J.R., Prince, R.C., Harner, E.J. and Atlas, R.M. (1994) Effectiveness of bioremediation for the Exxon Valdez oil spill. Nature 368(6470), 413-418.

Brody, T.M., Bianca, P.D. and Krysa, J. (2012) Analysis of inland crude oil spill threats, vulnerabilities, and emergency response in the midwest United States. Risk Analysis 32(10), 1741-1749.

Castiblanco, J.E., Carregosa, J.C., Santos, J.M. and Wisniewski, A. (2021) Molecular behavior assessment on initial stages of oil spill in terrestrial environments. Environmental Science Pollution Research 28, 13595-13604.

Caudle, K.L. and Maricle, B.R. (2014) Physiological relationship between oil tolerance and flooding tolerance in marsh plants. Environmental Experimental Botany 107, 7-14.

Caudle, K.L. and Maricle, B.R. (2015) Physiological and ecological effects of spilled motor oil on inland salt marsh communities: a mesocosm study. Wetlands 35, 501-507.

Chapman, H., Purnell, K., Law, R.J. and Kirby, M.F. (2007) The use of chemical dispersants to combat oil spills at sea: A review of practice and research needs in Europe. Marine Pollution Bulletin 54(7), 827-838.

Chen, Y., Zhou, Z., Wang, J., Zhao, Y. and Dou, Z. (2021a) Quantification and division of unfrozen water content during the freezing process and the influence of soil properties by low-field nuclear magnetic resonance. Journal of Hydrology 602, 126719.

Chen, Z., An, C., Fang, H., Zhang, Y., Zhou, Z., Zhou, Y. and Zhao, S. (2020) Assessment of regional greenhouse gas emission from beef cattle production: a case study of Saskatchewan in Canada. Journal of Environmental Management 264, 110443.

Chen, Z., An, C., Yin, J., Owens, E., Lee, K., Zhang, K. and Tian, X. (2021b) Exploring the use of cellulose nanocrystal as surface-washing agent for oiled shoreline cleanup. Journal of Hazardous Materials 402, 123464.

Chitra, N., Chandrasekaran, S., Srinivas, C.V., Athmalingam, S. and Venkatraman, B. (2022) Determination of soil porosity by a simple and novel technique of fusing thoron diffusion experiment and modeling. Journal of Radioanalytical and Nuclear Chemistry 331, 1-8.

Choo, H., Kim, J., Lee, W. and Lee, C. (2016) Relationship between hydraulic conductivity and formation factor of coarse-grained soils as a function of particle size. Journal of Applied Geophysics 127, 91-101.

Chu, L. and Fwa, T. (2019) Evaluation of surface infiltration performance of permeable pavements. Journal of Environmental Management 238, 136-143.

Chuvilin, E. and Miklyaeva, E. (2003) An experimental investigation of the influence of salinity and cryogenic structure on the dispersion of oil and oil products in frozen soils. Cold regions science and technology 37(2), 89-95.

Demand, D., Selker, J.S. and Weiler, M. (2019) Influences of macropores on infiltration into seasonally frozen soil. Vadose Zone Journal 18(1), 1-14.

Dhaka, A. and Chattopadhyay, P. (2021) A review on physical remediation techniques for treatment of marine oil spills. Journal of Environmental Management 288, 112428.

Dou, Z., Chen, Y., Zhuang, C., Zhou, Z. and Wang, J. (2022) Emergence of non-aqueous phase liquids redistribution driven by freeze-thaw cycles in porous media based on low-field NMR. Journal of Hydrology 612, 128106.

Eckle, P., Burgherr, P. and Michaux, E. (2012) Risk of large oil spills: a statistical analysis in the aftermath of Deepwater Horizon. Environmental science & technology 46(23), 13002-13008.

EPA, U.S. (2023) Types of Crude Oil.

Esteban, B., Riba, J.R., Baquero, G., Rius, A. and Puig, R. (2012) Temperature dependence of density and viscosity of vegetable oils. Biomass and bioenergy 42, 164-171.

Fan, Z., Hu, C., Zhu, Q., Jia, Y., Zuo, D. and Duan, Z. (2021) Three-dimensional pore characteristics and permeability properties of calcareous sand with different particle sizes. Bulletin of Engineering Geology the Environment 80, 2659-2670.

Feng, Q., An, C., Chen, Z. and Wang, Z. (2020) Can deep tillage enhance carbon sequestration in soils? A meta-analysis towards GHG mitigation and sustainable agricultural management. Journal of Hazardous Materials 133, 110293.

Fingas, M. (2002) The basics of oil spill cleanup, CRC press.

Fingas, M. (2011) An overview of in-situ burning. Oil Spill Science Technology, 737-903.

Fingas, M. and Fieldhouse, B. (2004) Formation of water-in-oil emulsions and application to oil spill modelling. Journal of Hazardous Materials 107(1-2), 37-50.

Freitas, B.L.S., Terin, U.C., Fava, N.d.M.N., Maciel, P.M.F., Garcia, L.A.T., Medeiros, R.C., Oliveira, M.d., Fernandez-Ibañez, P., Byrne, J. and Sabogal-Paz, L. (2022) A critical overview of household slow sand filters for water treatment. Water Research 208, 117870.

French-McCay, D.P., Jayko, K., Li, Z., Spaulding, M.L., Crowley, D., Mendelsohn, D., Horn, M., Isaji, T., Kim, Y.H. and Fontenault, J. (2021) Oil fate and mass balance for the Deepwater Horizon oil spill. Marine Pollution Bulletin 171, 112681.

Ge, J., Zhao, H.Y., Zhu, H.W., Huang, J., Shi, L.A. and Yu, S.H. (2016) Advanced sorbents for oil‐spill cleanup: recent advances and future perspectives. Advanced Materials 28(47), 10459-10490.

Gong, Y., Zhao, X., Cai, Z., O'reilly, S., Hao, X. and Zhao, D. (2014) A review of oil, dispersed oil and sediment interactions in the aquatic environment: influence on the fate, transport and remediation of oil spills. Marine Pollution Bulletin 79(1-2), 16-33.

Green, J. and Trett, M.W. (2012) The fate and effects of oil in freshwater, Springer Science & Business Media.

Grimaz, S., Allen, S., Stewart, J. and Dolcetti, G. (2008) Fast prediction of the evolution of oil penetration into the soil immediately after an accidental spillage for rapid-response purposes. Proceeding of 3rd International Conference on Safety & Environment in Process Industry, CISAP–3, Rome (I), 11-14.

Halmemies, S., Gröndahl, S., Nenonen, K. and Tuhkanen, T. (2003a) Estimation of the time periods and processes for penetration of selected spilled oils and fuels in different soils in the laboratory. Spill Science & Technology Bulletin 8(5-6), 451-465.

Halmemies, S., Gröndahl, S., Nenonen, K. and Tuhkanen, T. (2003b) Estimation of the time periods and processes for penetration of selected spilled oils and fuels in different soils in the laboratory. Spill Science Technology Bulletin 8(5-6), 451-465.

Hamilton, J.D. and Wu, J.C. (2014) Risk premia in crude oil futures prices. Journal of International Money Finance 42, 9-37.

Hangen, E., Buczko, U., Bens, O., Brunotte, J. and Hüttl, R. (2002) Infiltration patterns into two soils under conventional and conservation tillage: influence of the spatial distribution of plant root structures and soil animal activity. Soil Tillage Research 63(3-4), 181-186.

Hauptmann, A., Handle, K.F., Baloh, P., Grothe, H. and Loerting, T. (2016) Does the emulsification procedure influence freezing and thawing of aqueous droplets? Journal of Chemical Physics 145(21), 211923.

Hilpert, M. and Glantz, R. (2013) Exploring the parameter space of the Green–Ampt model. Advances in water resources 53, 225-230.

Hoehn, R., Stauffer, J., Masnik, M.T. and Hocutt, C. (1974) Relationships between sediment oil concentrations and the macroinvertebrates present in a small stream following an oil spill. Environmental Letters 7(4), 345-352.

Horton, R., Ankeny, M. and Allmaras, R. (1994) Effects of compaction on soil hydraulic properties. Developments in agricultural engineering 11, 141-165.

Hu, Y.T., Ting, Y., Hu, J.Y. and Hsieh, S.C. (2017) Techniques and methods to study functional characteristics of emulsion systems. Journal of food drug analysis 25(1), 16-26.

Huang, X., Andry, S., Yaputri, J., Kelly, D., Ladner, D.A. and Whelton, A. (2017) Crude oil contamination of plastic and copper drinking water pipes. Journal of Hazardous Materials 339, 385-394.

Hussein, M., Jin, M. and Weaver, J.W. (2002) Development and verification of a screening model for surface spreading of petroleum. Journal of Contaminant Hydrology 57(3-4), 281-302.

IPIECA and IOGP (2015) Oil spills: inland response.

ITOPF (2023) Oil Tanker Spill Statistics 2022, London, UK.

Iturbe, R., Flores, C., Castro, A. and Torres, L.G. (2007) Sub-soil contamination due to oil spills in six oil-pipeline pumping stations in northern Mexico. Chemosphere 68(5), 893-906.

Ivshina, I.B., Kuyukina, M.S., Krivoruchko, A.V., Elkin, A.A., Makarov, S.O., Cunningham, C.J., Peshkur, T.A., Atlas, R.M. and Philp, J.C. (2015) Oil spill problems and sustainable response strategies through new technologies. Environmental Science: Processes & Impacts 17(7), 1201-1219.

Japper-Jaafar, A., Bhaskoro, P. and Mior, Z. (2016) A new perspective on the measurements of wax appearance temperature: Comparison between DSC, thermomicroscopy and rheometry and the cooling rate effects. Journal of petroleum science Engineering 147, 672-681.

Ji, W., Boufadel, M., Zhao, L., Robinson, B., King, T. and Lee, K. (2021) Formation of oil-particle aggregates: Particle penetration and impact of particle properties and particle-to-oil concentration ratios. Science of the Total Environment 760, 144047.

Jiang, Z., Hutchinson, J. and Imrie, C.T. (2001) Measurement of the wax appearance temperatures of crude oils by temperature modulated differential scanning calorimetry. Fuel processing technology 80(3), 367-371.

Jiao, X., Shi, Q. and Gan, J. (2021) Uptake, accumulation and metabolism of PFASs in plants and health perspectives: A critical review. Critical reviews in environmental science and technology 51(23), 2745-2776.

John Jechura (2018) Crude Oil Assay –Hibernia (from ExxonMobil site), Colorado School of Mines.

Kale, R.V. and Sahoo, B. (2011) Green-Ampt infiltration models for varied field conditions: A revisit. Water resources management 25, 3505-3536.

Kane, D.L. and Stein, J. (1983) Water movement into seasonally frozen soils. Water Resources Research 19(6), 1547-1557.

Kaushik, G. (2015) Applied environmental biotechnology: Present scenario and future trends, Springer.

Khadanga, M., Mishra, R. and Sahu, B. (2022) Assessment of Pollution and Ecological Risk Index of Heavy Metals in the Surface Sediment of Estuary and the Coastal Environment of Bay of Bengal. Journal of Environmental Informatics 39(1), 35-48.

Kilpatrick, P.K. (2012) Water-in-crude oil emulsion stabilization: review and unanswered questions. Energy & Fuels 26(7), 4017-4026.

Klute, A. (1952) Some theoretical aspects of the flow of water in unsaturated soils. Soil Science Society of America Journal 16(2), 144-148.

Kök, M.V., Varfolomeev, M.A. and Nurgaliev, D.K. (2018) Wax appearance temperature (WAT) determinations of different origin crude oils by differential scanning calorimetry. Journal of petroleum science Engineering 168, 542-545.

Kruka, V., Cadena, E. and Long, T. (1995) Cloud-point determination for crude oils. Journal of Petroleum Technology 47(08), 681-687.

Kujawinski, E.B., Kido Soule, M.C., Valentine, D.L., Boysen, A.K., Longnecker, K. and Redmond, M.C. (2011) Fate of dispersants associated with the Deepwater Horizon oil spill. Environmental science & technology 45(4), 1298-1306.

La, Z. and Chai, L. (2021) Comprehensive study of evolution of global environmental quality research using informetric co-word network. Journal of Environmental Informatics 38(2), 116-130.

Lebedeva, E.V., Fogden, A., Senden, T.J. and Knackstedt, M.A. (2010) Kaolinite Wettability—The Effect of Salinity, pH and Calcium. Paper SCA 2010-11 presented at the 24th International Symposium of Core Analysts, Halifax, Canada, 4-7 October.

Lee, M. and Jung, J.-Y. (2015) Pollution risk assessment of oil spill accidents in Garorim Bay of Korea. Marine Pollution Bulletin 100(1), 297-303.

Levine, S., Bowen, B.D. and Partridge, S. (1989) Stabilization of emulsions by fine particles I. Partitioning of particles between continuous phase and oil/water interface. Colloids surfaces 38(2), 325-343.

Li, M., Yu, H., Zheng, D., Klemeš, J.J. and Wang, J. (2021) Effects of salt and solidification treatment on the oil-contaminated soil: A case study in the coastal region of Tianjin, China. Journal of Cleaner Production 312, 127619.

Lim, J., Wong, S., Law, M., Samyudia, Y. and Dol, S. (2015) A review on the effects of emulsions on flow behaviours and common factors affecting the stability of emulsions. Journal of Applied Sciences 15(2), 167-172.

Lin, C., He, G., Dong, C., Liu, H., Xiao, G. and Liu, Y. (2008) Effect of oil phase transition on freeze/thaw-induced demulsification of water-in-oil emulsions. Langmuir 24(10), 5291-5298.

Liu, J., Zhong, L., Lyu, C., Liu, Y. and Zhang, S. (2022) W/O emulsions generated by heavy oil in porous medium and its effect on re-emulsification. Fuel processing technology 310, 122344.

Liu, Y., Cui, Z., Huang, Z., López-Vicente, M. and Wu, G.-L. (2019) Influence of soil moisture and plant roots on the soil infiltration capacity at different stages in arid grasslands of China. Catena 182, 104147.

Lukyanets, Y. (2010) The Green and Ampt infiltration model accounting for air compression and air counterflow in the shallow water table environment: Laboratory experiments, University of South Florida.

Lynn, B., Medved, A. and Griggs, T. (2018) A comparative analysis on the impact of salinity on the heat generation of OTEC plants to determine the most plausible geographical location. PAM Review Energy Science & Technology 5, 119-130.

Maaref, S., Ayatollahi, S., Rezaei, N. and Masihi, M. (2017) The effect of dispersed phase salinity on water-in-oil emulsion flow performance: a micromodel study. Industrial engineering chemistry research 56(15), 4549-4561.

Majid, A.A., Saidian, M., Prasad, M. and Koh, C.A. (2015) Measurement of the water droplet size in water-in-oil emulsions using low field nuclear magnetic resonance for gas hydrate slurry applications. Canadian Journal of Chemistry 93(9), 1007-1013.

McCauley, C.A., White, D.M., Lilly, M.R. and Nyman, D.M. (2002a) A comparison of hydraulic conductivities, permeabilities and infiltration rates in frozen and unfrozen soils. Cold regions science and technology 34(2), 117-125.

McCauley, C.A., White, D.M., Lilly, M.R. and Nyman, D.M. (2002b) A comparison of hydraulic conductivities, permeabilities and infiltration rates in frozen and unfrozen soils. Cold Regions Science Technology 34(2), 117-125.

Meek, B., Rechel, E., Carter, L., DeTar, W. and Urie, A. (1992) Infiltration rate of a sandy loam soil: effects of traffic, tillage, and plant roots. Soil Science Society of America Journal 56(3), 908-913.

Mei, H., Li, Y., Lv, J., Chen, X., Lu, C., Suo, C. and Ma, Y. (2021) Development of an integrated method (MGCMs-SCA-FER) for assessing the impacts of climate change: a case study of Jing-Jin-Ji region. Journal of Environmental Informatics 38(2), 145-161.

Menon, V. and Wasan, D. (1988) Characterization of oil—water interfaces containing finely divided solids with applications to the coalescence of water-in-oil Emulsions: A review. Colloids surfaces 29(1), 7-27.

Merlin, F., Zhu, Z., Yang, M., Chen, B., Lee, K., Boufadel, M.C., Isaacman, L. and Zhang, B. (2021) Dispersants as marine oil spill treating agents: a review on mesoscale tests and field trials. Environmental Systems Research 10(1), 1-19.

Mohamed, A.I., Hussein, I.A., Sultan, A.S. and Al-Muntasheri, G.A. (2018) Use of organoclay as a stabilizer for water-in-oil emulsions under high-temperature high-salinity conditions. Journal of petroleum science Engineering 160, 302-312.

Mohler, R.E., Ahn, S., O'Reilly, K., Zemo, D.A., Devine, C.E., Magaw, R. and Sihota, N. (2020) Towards comprehensive analysis of oxygen containing organic compounds in groundwater at a crude oil spill site using GC× GC-TOFMS and Orbitrap ESI-MS. Chemosphere 244, 125504.

Moradi, M., Alvarado, V. and Huzurbazar, S. (2011) Effect of salinity on water-in-crude oil emulsion: evaluation through drop-size distribution proxy. Energy & Fuels 25(1), 260-268.

Napotnik, J.A., Baker, D. and Jellison, K.L. (2017) Effect of sand bed depth and medium age on Escherichia coli and turbidity removal in biosand filters. Environmental science & technology 51(6), 3402-3409.

Nelson, P.H. (2009) Pore-throat sizes in sandstones, tight sandstones, and shales. AAPG bulletin 93(3), 329-340.

Obu, J. (2021) How much of the earth's surface is underlain by permafrost? Journal of Geophysical Research: Earth Surface 126(5), e2021JF006123.

Oghenejoboh, K., Puyate, Y. and Abowei, M. (2008) Concentration distribution of spilled crude petroleum in different soils 2: Effects of volume of oil on spatial spread. Pollut. Res 27, 605-610.

Pal, R. (1996) Effect of droplet size on the rheology of emulsions. AIChE Journal 42(11), 3181-3190.

Panatdasirisuk, W., Liao, Z., Vongsetskul, T. and Yang, S. (2017) Separation of oil-in-water emulsions using hydrophilic electrospun membranes with anisotropic pores. Langmuir 33(23), 5872-5878.

Pang, S., Pu, W., Jiang, F., Gao, H., Wang, Y., Chen, Y. and Wei, P. (2021) Effect of water content on features of W/O emulsion during water flooding in heavy oil reservoir: Bulk properties and mobility control characteristics. Journal of petroleum science Engineering 207, 109075.

Paso, K., Silset, A., Sørland, G., Gon alves, M.d.A. and Sj blom, J. (2009) Characterization of the formation, flowability, and resolution of Brazilian crude oil emulsions. Energy & Fuels 23(1), 471-480.

Patel, H., Shah, S., Ahmed, R. and Ucan, S. (2018) Effects of nanoparticles and temperature on heavy oil viscosity. Journal of Petroleum Science and Engineering 167, 819-828.

Patterson, L.A., Konschnik, K.E., Wiseman, H., Fargione, J., Maloney, K.O., Kiesecker, J., Nicot, J.-P., Baruch-Mordo, S., Entrekin, S. and Trainor, A. (2017) Unconventional oil and gas spills: risks, mitigation priorities, and state reporting requirements. Environmental Science Technology 51(5), 2563-2573.

Pedersen, K.S. and Rønningsen, H.P. (2003) Influence of wax inhibitors on wax appearance temperature, pour point, and viscosity of waxy crude oils. Energy & Fuels 17(2), 321-328.

Qu, Z., An, C., Mei, Z., Yue, R., Zhao, S., Feng, Q., Cai, M. and Wen, J. (2022) An experimental and modeling study on the penetration of spilled oil into thawing frozen soil. Environmental Science: Processes Impacts 24(12), 2398-2408.

Qu, Z., An, C., Yue, R., Bi, H. and Zhao, S. (2023) Assessment of the infiltration of water-in-oil emulsion into soil after spill incidents. Science of The Total Environment, 165325.

Ramusino, M.C. and Zanzottera, D. (1986) Crude Dubai oil toxicity on some fresh-water invertebrates. Bull. Environ. Contam. Toxicol. 36(1).

Rawls, W.J., Brakensiek, D.L. and Miller, N. (1983) Green-Ampt infiltration parameters from soils data. Journal of hydraulic engineering 109(1), 62-70.

Savins, J. (1969) Non-Newtonian flow through porous media. Industrial Engineering Chemistry 61(10), 18-47.

Schmidt-Etkin, D. (2011) Oil spill science and technology, pp. 7-48, Elsevier.

Shen, J., Huang, G., An, C., Zhao, S. and Rosendahl, S. (2017) Immobilization of tetrabromobisphenol A by pinecone-derived biochars at solid-liquid interface: synchrotron-assisted analysis and role of inorganic fertilizer ions. Chemical Engineering Journal 321, 346-357.

Shi, S., Wang, Y., Liu, Y. and Wang, L. (2018) A new method for calculating the viscosity of W/O and O/W emulsion. Journal of petroleum science Engineering 171, 928-937.

Si-Zhong, Y., Hui-Jun, J., Zhi, W., Rui-Xia, H., Yan-Jun, J., Xiu-Mei, L. and Shao-Peng, Y. (2009) Bioremediation of oil spills in cold environments: a review. Pedosphere 19(3), 371-381.

Simmons, C.S. and Keller, J.M. (2005) Liquid Spills on Permeable Soil Surfaces: Experimental Confirmations. US Pacific Northwest National Lab (PNNL) Report.

Skryleva, E., Nikitin, V. and Dushin, V. (2020) Microgravity investigation of seepage flows in porous media. Advances in the Astronautical Sciences Conference, 729-739.

Smith, N.V., Saatchi, S.S. and Randerson, J.T. (2004) Trends in high northern latitude soil freeze and thaw cycles from 1988 to 2002. Journal of Geophysical Research: Atmospheres 109(D12).

Song, P., Huang, G., Hong, Y., An, C., Xin, X. and Zhang, P. (2020a) A biophysiological perspective on enhanced nitrate removal from decentralized domestic sewage using gravitational-flow multi-soil-layering systems. Chemosphere 240, 124868.

Song, S., Rong, L., Dong, K., Liu, X., Le Clech, P. and Shen, Y. (2020b) Particle-scale modelling of fluid velocity distribution near the particles surface in sand filtration. Water Research 177, 115758.

Soo, H. and Radke, C. (1986) A filtration model for the flow of dilute, stable emulsions in porous media—I. Theory. Chemical Engineering Science 41(2), 263-272.

Spaid, M.A. and Phelan Jr, F.R. (1997) Lattice Boltzmann methods for modeling microscale flow in fibrous porous media. Physics of fluids 9(9), 2468-2474.

Sreedeep, S. and Singh, D.N. (2011) Critical review of the methodologies employed for soil suction measurement. International Journal of Geomechanics 11(2), 99-104.

Stalcup, D., Yoshioka, G., Mantus, E. and Kaiman, B. (1997) Characteristics of oil spills: inland versus coastal, pp. 939-940, American Petroleum Institute.

Steinwinder, J. and Beckingham, L.E. (2019) Role of pore and pore-throat distributions in controlling permeability in heterogeneous mineral dissolution and precipitation scenarios. Water Resources Research 55(7), 5502-5517.

Sundar, S., Mishra, A. and Shukla, J. (2021) Effects of mitigation options on the control of methane emissions caused by rice paddies and livestock populations to reduce global warming: a modeling study and comparison with environmental data. Journal of Environmental Informatics 38(2), 106-115.

Taraneh, J.B., Rahmatollah, G., Hassan, A. and Alireza, D. (2008) Effect of wax inhibitors on pour point and rheological properties of Iranian waxy crude oil. Fuel processing technology 89(10), 973-977.

Thomas, M.J., Collinge, E., Witt, M., Lozano, D.C.P., Vane, C.H., Moss-Hayes, V. and Barrow, M.P. (2019) Petroleomic depth profiling of Staten Island salt marsh soil: 2ω detection FTICR MS offers a new solution for the analysis of environmental contaminants. Science of the Total Environment 662, 852-862.

Tian, H., Wei, C., Wei, H. and Zhou, J. (2014) Freezing and thawing characteristics of frozen soils: Bound water content and hysteresis phenomenon. Cold regions science and technology 103, 74-81.

Troisi, G., Barton, S. and Bexton, S. (2016) Impacts of oil spills on seabirds: Unsustainable impacts of non-renewable energy. International Journal of Hydrogen Energy 41(37), 16549-16555.

Valikhan Anaraki, M., Mahmoudian, F., Nabizadeh Chianeh, F. and Farzin, S. (2022) Dye Pollutant Removal from Synthetic Wastewater: A New Modeling and Predicting Approach Based on Experimental Data Analysis, Kriging Interpolation Method, and Computational Intelligence Techniques. Journal of Environmental Informatics 40(2), 84-94.

Vandermeulen, J.H. and Ross, C.W. (1995) Oil spill response in freshwater: assessment of the impact of cleanup as a management tool. Journal of Environmental Management 44(4), 297-308.

Vanloocke, R., De Borger, R., Voets, J. and Verstraete, W. (1975) Soil and groundwater contamination by oil spills; problems and remedies. International Journal of Environmental Studies 8(1-4), 99-111.

Venosa, A.D., Campo, P. and Suidan, M.T. (2010) Biodegradability of lingering crude oil 19 years after the Exxon Valdez oil spill. Environmental science & technology 44(19), 7613-7621.

Vergeynst, L., Greer, C.W., Mosbech, A., Gustavson, K., Meire, L., Poulsen, K.G. and Christensen, J.H. (2019) Biodegradation, photo-oxidation, and dissolution of petroleum compounds in an Arctic Fjord during summer. Environmental science & technology 53(21), 12197-12206.

Visintin, R.F., Lockhart, T.P., Lapasin, R. and D'Antona, P. (2008) Structure of waxy crude oil emulsion gels. Journal of Non-Newtonian Fluid Mechanics 149(1-3), 34-39.

Wan, X., Lai, Y. and Wang, C. (2015) Experimental study on the freezing temperatures of saline silty soils. Permafrost and Periglacial Processes 26(2), 175-187.

Wang, H., Zhu, X., Zakari, S., Chen, C., Liu, W. and Jiang, X.-J. (2022a) Assessing the Effects of Plant Roots on Soil Water Infiltration Using Dyes and Hydrus-1D. Forests 13(7), 1095.

Wang, Z., An, C., Lee, K., Owens, E., Boufadel, M. and Feng, Q. (2022b) Dispersion modeling of particulate matter from the in-situ burning of spilled oil in the northwest Arctic area of Canada. Journal of Environmental Management 301, 113913.

Wang, Z., An, C., Lee, K., Owens, E., Chen, Z., Boufadel, M., Taylor, E. and Feng, Q. (2021) Factors influencing the fate of oil spilled on shorelines: a review. Environmental Chemistry Letters 19, 1611-1628.

Weidhaas, J.L., Dietrich, A.M., DeYonker, N.J., Ryan Dupont, R., Foreman, W.T., Gallagher, D., Gallagher, J.E., Whelton, A.J. and Alexander, W.A. (2016) Enabling Science Support for Better Decision-Making When Responding to Chemical Spills. Journal of Environmental Quality 45(5), 1490-1500.

Weiss, J. and Muschiolik, G. (2007) Factors affecting the droplet size of water-in-oil emulsions (W/O) and the oil globule size in water-in-oil-in-water emulsions (W/O/W). Journal of Dispersion Science Technology 28(5), 703-716.

Wilson, M., Hale, C., Maung-Douglass, E., Partyka, M., Sempier, S. and Skelton, T. (2019) Impacts of oil on mangroves. Gulf of Mexico Research Initiative.

Wong, S., Lim, J. and Dol, S. (2015) Crude oil emulsion: A review on formation, classification and stability of water-in-oil emulsions. Journal of petroleum science Engineering 135, 498-504.

Xin, Q., Hounjet, L.J. and Hartwell, A. (2022) Spill behaviours of pipeline-transportable processed bitumen products in fresh water. Fuel processing technology 309, 122040.

Xin, X., Huang, G., An, C. and Feng, R. (2019) Interactive toxicity of triclosan and nano-TiO2 to green alga Eremosphaera viridis in Lake Erie: A new perspective based on Fourier transform infrared spectromicroscopy and synchrotron-based X-ray fluorescence imaging. Environmental science & technology 53(16), 9884-9894.

Xu, G., Zheng, Q., Yang, X., Yu, R. and Yu, Y. (2021) Freeze-thaw cycles promote vertical migration of metal oxide nanoparticles in soils. Science of the Total Environment 795, 148894.

Xuwen, Q., Cheng, L., Pingkang, W. and Qianyong, L. (2022) Hydrate phase transition and seepage mechanism during natural gas hydrate production tests in the South China Sea: A review and prospect. China Geology 5(2), 201-217.

Yadav, D., Singh, R., Kumar, A. and Sarkar, B. (2022) Reduction of Pollution through Sustainable and Flexible Production by Controlling By-Products. Journal of Environmental Informatics 40(2), 106-124.

Yan, N., Gray, M.R. and Masliyah, J.H. (2001) On water-in-oil emulsions stabilized by fine solids. Colloids Surfaces A: Physicochemical Engineering Aspects 193(1-3), 97-107.

Yang, H., Rahardjo, H., Leong, E.C. and Fredlund, D.G. (2004) A study of infiltration on three sand capillary barriers. Canadian Geotechnical Journal 41(4), 629-643.

Yang, K., Zhu, L. and Xing, B. (2006) Enhanced soil washing of phenanthrene by mixed solutions of TX100 and SDBS. Environmental science & technology 40(13), 4274-4280.

Yao, R., Yang, J., Wang, X., Zhao, Y., Li, H., Gao, P., Xie, W. and Zhang, X. (2022) Improving Soil Salinity Simulation by Assimilating Electromagnetic Induction Data into HYDRUS Model Using Ensemble Kalman Filter. Journal of Environmental Informatics 39(2), 81-96.

Yao, Y., Huang, G., An, C., Cheng, G. and Wei, J. (2017) Effects of freeze–thawing cycles on desorption behaviors of PAH-contaminated soil in the presence of a biosurfactant: a case study in western Canada. Environmental Science: Processes & Impacts 19(6), 874-882.

Yin, J.H. (2009) Influence of relative compaction on the hydraulic conductivity of completely decomposed granite in Hong Kong. Canadian Geotechnical Journal 46(10), 1229-1235.

Yoshioka, G. and Carpenter, M. (2002) Characteristics of reported inland and coastal oil spills. US Environmental Protection Agency Report.

Yuan, Z., Xu, J., Chen, J., Wang, Y. and Yin, J. (2022) EVI Indicated Spatial-Temporal Variations in Vegetation and Their Responses to Climatic and Anthropogenic Factors in the Chinese Mainland Since 2000s. Journal of Environmental Informatics 40(2), 157-157.

Yue, R., An, C., Ye, Z., Li, X., Li, Q., Zhang, P., Qu, Z. and Wan, S. (2023a) A pH-responsive phosphoprotein washing fluid for the removal of phenanthrene from contaminated peat moss in the cold region. Chemosphere 313, 137389.

Yue, R., Ye, Z., Gao, S., Cao, Y., Lee, K., An, C., Qu, Z. and Wan, S. (2023b) Exploring the use of sodium caseinate-assisted responsive separation for the treatment of washing effluents in shoreline oil spill response. Chemosphere 873, 162363.

Yuhua, D. and Datao, Y. (2005) Estimation of failure probability of oil and gas transmission pipelines by fuzzy fault tree analysis. Journal of Loss Prevention in the Process Industries 18(2), 83-88.

Zhang, B., Matchinski, E.J., Chen, B., Ye, X., Jing, L. and Lee, K. (2019) World seas: an environmental evaluation, pp. 391-406, Elsevier.

Zhao, S., Huang, G., An, C., Wei, J. and Yao, Y. (2015) Enhancement of soil retention for phenanthrene in binary cationic gemini and nonionic surfactant mixtures:

Characterizing two-step adsorption and partition processes through experimental and modeling approaches. Journal of Hazardous Materials 286, 144-151.

Zhao, Y., Yu, B., Yu, G. and Li, W. (2014) Study on the water-heat coupled phenomena in thawing frozen soil around a buried oil pipeline. Applied thermal engineering 73(2), 1477-1488.

Zolfaghari, R., Fakhru'l-Razi, A., Abdullah, L.C., Elnashaie, S.S. and Pendashteh, A. (2016) Demulsification techniques of water-in-oil and oil-in-water emulsions in petroleum industry. Separation purification technology 170, 377-407.

PUBLICTIONS

Peer-reviewed journal articles

(1) **Qu, Z.**, An, C., Yue, R., Bi, H., & Zhao, S., Assessment of the Infiltration of Water-in-oil Emulsion into Soil After Spill Incidents. Science of The Total Environment (*Elsevier*), 896, 165325 (2023)

(2) **Qu, Z.**, An, C., Mei, Z., Yue, R., Zhao, S., Feng, Q., Cai, M. and Wen, J., An Experimental and Modeling Study on the Penetration of Spilled Oil into Thawing Frozen Soil. Environmental Science: Impacts and Processes (*Royal Society of Chemistry*), 24, 2398-2408 (2022)

(3) Yue, R., An, C., Ye, Z., Li, X., Li, Q., Zhang, P., **Qu, Z.** and Wan, S., A pH-Responsive Phosphoprotein Washing Fluid for the Removal of Phenanthrene from Contaminated Peat Moss in the Cold Region. Chemosphere (*Elsevier*), 313, 137389 (2022)

(4) Wan, S., Yang, X., Chen, X., **Qu, Z.**, An, C., Zhang, B., Lee, K. and Bi, H., Emerging Marine Pollution from Container Ship Accidents: Risk Characteristics, Response Strategies, and Regulation Advancements. Journal of Cleaner Production (*Elsevier*), 376, 134266 (2022).

Conference abstracts

(1) **Qu, Z.**, An, C., Yue, R., Penetration of Spilled Oil into Thawing Frozen Soil. PEOPLE 2023 – Collaborative Solutions to Environmental Problems under Climate Change, August 7-11, 2023, Montreal, Canada.

(2) **Qu, Z.**, An, C., Yue, R., Oil Penetration into Thawing Frozen Soil after Spill Accidents, INQ's Northern Days, June 5-6, 2023, Trois-Rivières, Canada